Cytotherapy 27 (2025) 917–932

Contents lists available at ScienceDirect

FULL-LENGTH ARTICLE

CYTOTHERAPY

journal homepage: www.isct-cytotherapy.org

International Society ISCT Cell & Gene Therapy®

Immunotherapy

Mannan-targeting chimeric antigen receptor redirected antifungal activity of NK-92 cells against *Candida albicans*

Gabriela Yamazaki de Campos[1,2], Júlia Garcia Guimarães[1], Michele Procópio Machado[2], Patrícia Kellen Martins Oliveira-Brito[2], Ben Shin[3], Antonio Di Maio[4], Douglas dos-Santos[2], Patricia Vianna Bonini Palma[5], Thaila Fernanda dos Reis[6], Gustavo Henrique Goldman[6,7], Angelina S. Palma[8], Steve J. Matthews[3], Ten Feizi[4], Yan Liu[4], Thiago Aparecido da Silva[1,2,7,*]

[1] Department of Clinical Analysis, School of Pharmaceutical Sciences in Araraquara, Sao Paulo State University, Araraquara, São Paulo, Brazil
[2] Department of Cell and Molecular Biology and Pathogenic Bioagents, Ribeirão Preto Medical School, University of São Paulo, Ribeirão Preto, São Paulo, Brazil
[3] Department of Life Sciences, Imperial College London, London, United Kingdom
[4] Department of Metabolism, Digestion and Reproduction, Imperial College London, London, United Kingdom
[5] Regional Blood Center, Ribeirão Preto, São Paulo, Brazil
[6] School of Pharmaceutical Sciences of Ribeirão Preto, University of São Paulo, Ribeirão Preto, São Paulo, Brazil
[7] National Institute of Science and Technology in Human Pathogenic Fungi, Brazil
[8] UCIBIO, Applied Molecular Biosciences Unit, Department of Chemistry, School of Science and Technology, NOVA University Lisbon, Caparica, Portugal
*Correspondence: Thiago Aparecido da Silva, PhD, Clinical Hematology Lab. Rodovia Araraquara Jau, Km 01 - S/N - Campos Ville, Araraquara, 14800-903, São Paulo, Brazil. *E-mail address:* thiago-aparecido.silva@unesp.br (T.A. da Silva).

A B S T R A C T

Chimeric antigen receptors (CARs) offer promising prospects for innovative cell-based therapies against invasive fungal infections such as invasive candidiasis. Here, we have developed 4 CARs targeting *Candida albicans* with distinct single-chain variable fragments (scFvs): scFv3-CAR, scFv5-CAR, scFv12-CAR, and scFvκ3-1-CAR. In T cells, scFv5-CAR induced IL-2 expression in response to *C. albicans* hyphae, while scFv3-CAR and scFv12-CAR did not mediate cell activation against *C. albicans*. Notably, scFvκ3-1-CAR mediated the strongest cell activation against *C. albicans* yeast, hyphae, and other clinically relevant *Candida* species. scFvκ3-1-CAR-NK-92 cells exhibited elevated IFN-γ and CD107a expression, reducing *C. albicans* viability. NOD scid gamma (NSG) mice treated with scFvκ3-1-CAR-NK-92 cells had reduced *C. albicans* burden in the kidneys 24 hours postinfection. We showed that scFvκ3-1-CAR targets *C. albicans* mannan but no other glycans in glycan microarray screening analyses. These findings reveal the scFvκ3-1-CAR potential as a therapeutic strategy for treating *Candida* spp. by modifying peripheral blood mononuclear cells.

Key Words: chimeric antigen receptor, invasive candidiasis, CAR-T cells, CAR-NK cells, mannan, *Candida albicans*.

Introduction

Candida spp. are commensal organisms that reside in the gastrointestinal tract and on the skin and can cause invasive candidiasis by spreading from their natural colonization sites to the bloodstream, leading to systemic dissemination [1]. Approximately 1,565,000 individuals are affected by candidemia or invasive candidiasis annually, resulting in 995,000 deaths (63.6%) [2]. Although *Candida albicans* remains the predominant species responsible for these infections, other species, such as *Candida auris, Candida glabrata* (*Nakaseomyces glabratus*), *Candida tropicalis, Candida parapsilosis,* and *Candida krusei,* also contribute to the occurrence of candidiasis [1,3,4].

Various microenvironmental factors in the host induce the transition from the yeast form to the hyphal form of *C. albicans*, which involves the regulation of genes encoding proteins and glycosyltransferases involved in the cell wall composition, facilitating the evasion of *Candida* spp. from the host immune response [5–7]. The cell wall of *Candida* spp. is a virulence factor that plays an essential role in the pathobiology of candidemia, functioning as both a protective barrier and a key interface with the host immunity. In *C. albicans*, it is composed predominantly of carbohydrates (80–90%), with an outer layer rich in N- and O-linked mannose polymers and an inner layer primarily formed by β-1,3-glucan and β-1,6-glucan [8]. These glycans' diversity expressed by *C. albicans* and other fungi have been

https://doi.org/10.1016/j.jcyt.2025.05.001

considered as pathogen-associated molecular patterns (PAMPs) potentially recognized by pattern recognition receptors (PRRs) on innate immune cells, triggering their activation, including natural killer (NK) cells [9]. NK cells play a crucial role in controlling *C. albicans* filament growth in the initial hours of infection, which is achieved through the release of cytotoxic granules such as perforins and granzymes [10]. Additionally, NK cells release interferon- γ (IFN-γ), tumor necrosis factor- α (TNF-α), granulocyte-macrophage colony-stimulating factor (GM-CSF), and chemokines for NK cell migration, and IFN-γ production activates polymorphonuclear leukocytes, increasing antifungal activity and promoting T-cell differentiation [11]. The differentiation of $CD4^+$ T-helper (Th) and $CD8^+$ T-cytotoxic (Tc) cells is crucial for inhibiting the growth of *C. albicans* hyphae *in vitro* [12], and the cytotoxic activity of $CD8^+$ T cells, which involves cytolytic granules and proinflammatory mediators, is necessary for combating invasive candidiasis [13]. Failure of these cells to drive adaptive immune responses to *C. albicans* may be associated with structural remodeling of the *C. albicans* cell wall.

Immunotherapy strategies, including adoptive T- and NK-cell therapies, show promise for treating invasive fungal infections (IFIs) and hold potential for clinical translation [14]. In this context, chimeric antigen receptor (CAR) technology has emerged as a promising approach, as demonstrated by previous studies [15–20]. CARs are receptors designed to be expressed by immune cells, redirecting them to interact with a specific antigen (protein, glycoprotein, carbohydrates, lipids, and others) localized on the cell surface. The antigen-binding domain of a CAR consists of a single-chain variable fragment (scFv) derived from a monoclonal antibody specific to the target antigen [21]. CARs also include a transmembrane domain, often derived from CD28 or CD8 molecules, which anchors the receptor to the cell surface. The signaling domain of a second-generation CAR is composed of activation motifs from the CD3ζ chain coupled with a costimulatory molecule (such as CD28, 4-1BB, or iCOS) [21]. Over the past decade, human T cells have been engineered with CARs to target *Aspergillus fumigatus* conidia and/or hyphae [18,20]. Our group developed a CAR to target *Cryptococcus* spp. capsules [15–17]) and a CAR to target *C. albicans* [22]. These novel CARs were evaluated in human T cells, and promising antifungal activity was demonstrated. However, CAR-engineered NK cells remain largely unexplored for the treatment of IFIs. Given their proven efficacy in cancer immunotherapy and the clinical use of the NK-92 cell line as an off-the-shelf therapy [23], NK cells represent a platform for the development of CAR-based strategies against IFIs.

To advance the application of CAR technology for fungal targeting, this study focused on developing CARs capable of redirecting T and NK cells (Jurkat and NK-92 lines) to recognize the *Candida* species cell wall. scFvs previously described in the literature and derived from human monoclonal antibody fragments generated by phage display against *Candida* species were selected to generate novel CARs, as follows: scFv3 recognizes the adhesin Als3p, a protein associated with germ tube and hyphal formation [24]; scFv5 recognizes the *SPT6* gene product [25]; scFv12 binds to a protein (unknown) [26]; and scFvκ3-1 recognizes a carbohydrate (unknown) [27]. scFvκ3-1-CAR can be highlighted as a novel CAR containing a fine specificity to polysaccharides of mannoproteins from yeast and hyphal forms of *C. albicans*. This study pioneers the bioengineering of CAR-NK-92 cells to target and damage *C. albicans*, opening new perspectives to enhance the fungicidal activity of human primary T and NK cells against *Candida* species.

Materials and Methods

Chemicals and reagents

Chemicals and reagents for cell culture were obtained from Thermo Fisher Scientific (sodium pyruvate, XTT), Sigma–Aldrich (Saint Louis, MO, USA; penicillin–streptomycin, dasatinib, ionomycin, folic acid, myoinositol, menadione, curdlan, mannan), Gibco (Waltham, MA, USA; MEM-alpha, fetal bovine serum, horse serum, phosphate buffer saline [PBS], 2-mercaptoethanol), and Corning (Manassas, VA, USA; RPMI 1640, high-glucose Dulbecco's Minimal Essential Medium [DMEM]). Reagents for the fungal culture experiments were obtained from KASVI (Madri, Spain; Sabouraud dextrose), Sigma–Aldrich (agar, CFW), and AppliChem (Darmstadt, Germany; kanamycin). Reagents and chemicals for flow cytometry, microscopy, and biological activity assays were obtained from BD Biosciences (San Diego, CA, USA; Fixation/Permeabilization Kit, monensin, cytokine kit, Annexin V cat. 556422, anti-CD25 [cat. 555432], anti-CD69 [cat. 555531], anti-TIM3 [cat. 563422], anti-PD-1 [cat. 560795], anti-phosZAP70 [cat. 557881], anti-CD107 [cat. 555801] antibodies), Sigma–Aldrich (propidium iodide, anti-FLAG, phycoerythrin-conjugated streptavidin), and InvivoGen (San Diego, CA, USA; R406 inhibitor, β-glucan peptide). The transfection reagent and lentiviral particle concentration solution were obtained from Invitrogen (Carlsbad, CA, USA; Lipofectamine 3000) and Takara (Mountain View, CA, USA; Lenti-X concentrator), respectively.

Cell lines and growth conditions

HEK-293T and Jurkat cell lines were obtained from the Rio de Janeiro Cell Bank (BCRJ). The NK-92 cell line was was acquired from the American Type Culture Collection (ATCC). HEK-293T cells were cultured in high-glucose DMEM supplemented with fetal bovine serum (10%), sodium pyruvate (100 mM), and penicillin–streptomycin (1%). Jurkat cells were cultured in RPMI 1640 medium supplemented with fetal bovine serum (10%), sodium pyruvate (100 mM), and penicillin–streptomycin (1%). NK-92 cells were cultivated in minimum essential medium (MEM) supplemented with fetal bovine serum (12,5%), horse serum (12,5%), penicillin–streptomycin (1%), 2-mercaptoethanol (55 mM), folic acid (7 μg/mL), myoinositol (36 μg/mL) and interleukin-2 (IL-2; 200 U/mL). Cells were cultured in a humidified atmosphere with 5% CO_2 at 37°C.

Animals

Nine-week-old female and male NSG mice were maintained in the animal facility situated at the Blood Center of the Ribeirão Preto Medical School of the University of São Paulo, Brazil. To perform the animal studies, the mice were housed at the Department of Cell and Molecular Biology and Pathogenic Bioagents of the Ribeirão Preto Medical School, and animal procedures were conducted according to the Ethical Principles Guide for the Care and Use of Laboratory Animals adopted by the Brazilian College of Animal Experimentation. The Committee on Ethics in Animal Research of the Ribeirão Preto Medical School approved this study (protocol 071/2021). The animals were housed under controlled environmental conditions at ambient temperature and humidity and maintained on a 12-hour light cycle. The mice were provided *ad libitum* access to chow and water. The mice were anesthetized by administration of ketamine hydrochloride (20.0 mg/kg, intraperitoneal) and xylazine hydrochloride (2 mg/kg, intraperitoneal) before euthanasia after the *C. albicans* infection period.

Culture of Candida *spp. and* Cryptococcus *spp. and heat killing of yeast and/or hyphal and pseudohyphal forms*

Candida albicans (ATCC 64548), *Candida parapsilosis* (ATCC 90018), *Candida tropicalis* (H2747), *Candida glabrata* (H3479), *Candida krusei* (ATCC 6258), *Candida guilliermondii* (ATCC 22017), *Candida auris* (clinical isolates 467, 468, and 469), *Cryptococcus gattii* (R265), *Cryptococcus neoformans* (H99) and *Cryptococcus neoformans* (acapsular mutant, CAP67) were recovered from 25% v/v glycerol stocks stored at −80°C. The fungi were spread on Sabouraud dextrose agar, and after 24 hours of incubation at 30°C, the yeasts were inoculated into Sabouraud dextrose broth and were agitated at 150 rpm at 30°C for

16 hours. The yeasts were harvested by centrifugation at 7600 × g for 10 minutes at 25°C and washed twice with sterile PBS. Cell concentration was determined using a Neubauer chamber. The yeast-to-hyphal/pseudohyphal form transition was achieved by seeding 2×10^5 yeast cells/mL (4×10^4 yeast cells/well) in 96-well plates containing RPMI-1640 or MEM. The yeast cells were incubated at 37°C for 3 to 4 hours, and the transition stage was monitored and confirmed using an inverted microscope. Heat killing of hyphal and pseudohyphal forms was performed by heating 70°C for 1 hour. The cell culture supernatants were replaced with the fresh medium before adding Jurkat or NK-92 cells modified with or without CAR. *Candida* spp. and *Cryptococcus* spp. yeast forms were inactivated at 70°C for 1 hour. The yeast cells were washed twice with sterile PBS before cell counting using a Neubauer chamber.

CAR construction

The antigen binding domain, hinge/transmembrane domain, and signal transduction regions that compose the CAR were synthesized by GenScript and inserted into a lentiviral plasmid backbone (pLenti-Cas9-EGFP, GenScript, NJ, USA) using AfeI/BamHI restriction sites, and the *GFP* reporter gene was inserted into the CAR reading frame. The scFvs in the antigen binding domain were derived from monoclonal antibody fragments previously described [24,26,27], which generated scFv3-CAR, scFv5-CAR, scFv12-CAR, and scFvκ3-1-CAR constructs. The hinge/transmembrane domain was composed of the CD8 molecule (UniProt P01732, 136–206 aa position) and the cytoplasmic portion of the human CD137 molecule (UniProt Q07011, 214–255 aa position) coupled to the cytoplasmic region of the human CD3ζ molecule (UniProt P20963, 52–164 aa position). The scFv3-CAR, scFv5-CAR, and scFv12-CAR each contained a FLAG tag in the N-terminus. The mock construct was a plasmid backbone containing the GFP sequence alone and served as a control lentiviral (pLenti-mock) empty vector.

Production of lentiviral particles

HEK-293T cells (2×10^6 cells/flask) were dispensed in 25 cm^2 cell culture flasks to produce lentiviral particles containing the plasmid encoding CAR. The cells were cotransfected with the accessory plasmids pMD2. G (VSV-G envelope-expressing plasmid—1 μg/flask), psPAX2 (lentiviral packaging plasmid—1.5 μg/flask), and each CAR-vector plasmid (2.5 μg/flask) using Lipofectamine 3000 following the manufacturer's instructions. The cell culture supernatant was collected every 24 hours and replaced with fresh medium during 72 hours, and the lentiviral particles were concentrated using Lenti-X concentrator reagent according to the manufacturer's instructions. The lentiviral particles diluted in PBS were frozen at −80°C, and the titer of the lentiviral particles was determined in Jurkat cells using a spinoculation protocol (850 × g for 65 min at RT) as previously reported [17]. The formula {[(%GFP/100) × dilution × cell seeded]/final volume} was used to calculate the titer of lentiviral particles expressed as transducing units per mL (TU/mL).

Generation of CAR-expressing Jurkat and NK-92 cells

Jurkat or NK-92 cells (1×10^5 cells/250 μL/well) were seeded in 48-well plates containing appropriate medium, and cell transduction was performed using a spinoculation protocol (850 × g, at room temperature, for 65 min). Jurkat cells were modified with pLenti-mock, scFv3-, scFv12-, or scFvκ3-1-CAR at an MOI of 5 or with scFv5-CAR at a multiplicity of infection (MOI) of 10. NK-92 cells were modified with scFvκ3-1-CAR at an MOI of 10. Immediately after transduction, the modified cells were incubated in a humidified atmosphere with 5% CO_2 at 37°C for 72 hours. The transduction efficiency was evaluated using flow cytometry with GFP expression as a reporter. The cell concentration and viability were determined using propidium iodide (PI; 10 μg/mL) staining. Jurkat and NK-92 cells expressing CAR were expanded for 7 days and were enriched using fluorescence-activated cell sorting (FACS), which isolated a cell population expressing high levels of GFP. The sorted cells were expanded to create a cell stock containing Jurkat and NK-92 cells modified with CAR or pLenti-mock.

Detection of CAR expression on the cell surface

The expression of scFv3-, scFv5-, and scFv12-CAR on the surface of Jurkat cells was detected by the presence of a FLAG-tag in the N-terminus of the CAR. Cells modified with pLenti-mock were used as a negative control. Jurkat cells (1×10^6 cells/tube) were pelleted (300 × g, 10 min, 4°C) and blocked with 0.5% bovine serum albumin/phosphate buffer saline (BSA/PBS) for 30 minutes. The cells were washed twice with PBS and incubated with an anti-FLAG monoclonal antibody (5 μg/mL; Sigma Aldrich) for 30 minutes. The cells were washed with PBS and incubated with a biotinylated goat secondary antibody. The detection of CAR was using streptavidin–phycoerythrin (PE) at a dilution of 1:100. After 30 minutes of incubation, the cells were washed and resuspended in PBS, and the percentage of cells positive for FLAG was measured by flow cytometry (Guava Easycyte Mini). All the incubations were performed on ice.

Incubation of CAR-expressing Jurkat and NK-92 cells with Candida *spp. or carbohydrates*

Jurkat cells (2×10^5/mL) or NK-92 cells (5×10^5/mL) expressing CAR were dispensed into 96-well plates containing live or HK yeast cells and hyphae that were cocultured with different ratios of target (T) to effector (E) cells. Jurkat cells were cocultured at a T:E ratio of 1:1 for HK yeast cells and hyphae and 1:100, 1:200, and 1:400 for live yeast cells. The NK-92 cells were cocultured at a T:E ratio of 1:50, 1:100, or 1:200 relative to live yeast cells. In addition, Jurkat cells modified with or without CAR were incubated with mannan from *Saccharomyces cerevisiae* (1 μg/mL), beta-glucan (1 μg/mL), curdlan (1 μg/mL), a cell wall protein extract of *C. albicans* (1 μg/mL), phorbol 12-myristate 13-acetate (PMA; 50 ng/mL) plus ionomycin (1 μM), or phytohemagglutinin (PHA-L; 5 μg/mL) + PMA (50 ng/mL) as positive controls. Jurkat cells transduced with mock were used as a negative control for cell activation. Cells were incubated in a humidified atmosphere with 5% CO_2 at 37°C for 24 hours and harvested to detect the expression of exhaustion and activation markers by flow cytometry, as described in the next section. The levels of cytokines in the cell culture supernatants were measured by enzyme-linked immunoassay (ELISA). The levels of IL-2 (BD OptiEIA Human IL-2 kit) and IFN-γ (BD OptiEIA Human IFN-γ kit) in the supernatant indicated the cell activation of Jurkat and NK-92 cells, respectively.

Detection of exhaustion and activation markers on the cell surface and intracellular staining for phospho-ZAP-70 by flow cytometry

The expression of exhaustion markers (PD-1 and TIM-3) and activation markers (CD25 and CD69) was evaluated in Jurkat cells expressing or not expressing CAR. The HK yeast or hyphae of *C. albicans* were cocultured with modified Jurkat cells as described above and the cells incubated with medium only were used as a negative control. The cocultures were incubated in a humidified atmosphere with 5% CO_2 at 37°C; after 24 hours of incubation, the cells were collected to detect PD-1, TIM-3, CD25, or CD69. The cells were blocked with 1% BSA/PBS for 30 minutes and washed with PBS. The cells were incubated with anti-PD-1, anti-TIM-3, anti-CD25, or anti-CD69 monoclonal antibodies for 30 minutes and washed. The percentage of positive cells was measured by flow cytometry (Guava Easycyte Mini). The incubation and washing steps were performed at 4°C.

Jurkat cells expressing scFvκ3-1-CAR or mock cells (2×10^5 cells/mL) were seeded in a 96-well plate and incubated with medium alone, HK yeast cells, or with the hyphae of *C. albicans* at an E:T ratio of 1:1. After 10 minutes of incubation, the cells were harvested and pelleted ($300 \times$ g, 10 min, at 4°C) before the addition of fixation/permeabilization solution, according to the manufacturer's instructions. The cells were incubated with an anti-phospho-ZAP70 monoclonal antibody for 45 minutes and washed once before the percentage of cells positive for phosphor-ZAP-70 was determined by flow cytometry (Guava Easycyte Mini). The phosphorylation of ZAP-70 was induced with H_2O_2 (0.03%) as a positive control. All incubation and washing steps were performed at 4°C.

Fluorescence microscopy to monitor the redirection of modified cells to target C. albicans

HK yeast cells and hyphae (2×10^5 cells/mL) were stained with CFW (100 μg/mL) for 1 hour and washed once before incubation with mock or scFvκ3-1-CAR Jurkat cells (2×10^5 cells/mL) in a 96-well plate. The coculture was incubated in a humidified atmosphere with 5% CO_2 at 37°C for 24 hours, and the targeting of the yeast cells and hyphae (blue) by modified Jurkat cells (green) was visualized under a fluorescence microscope (Leica) at 200× magnification. The interactions between NK-92 cells (5×10^5 cells/mL) modified or not modified with scFvκ3-1-CAR and *C. albicans* were also analyzed by fluorescence microscopy. Live *C. albicans* yeast cells were incubated with modified NK-92 cells in a 96-well plate at ratios of target to effector of 1:50 and 1:100. After 6 hours of incubation, CFW (10 μg/mL) was added to the coculture for labeling of *C. albicans* for 15 minutes before visualization under a fluorescence microscope (Leica) at 200× magnification.

Effects of the pharmacologic inhibitors dasatinib and R406 on cell activation mediated by the scFvκ3-1-CAR

Jurkat cells expressing scFvκ3-1-CAR and mock cells (2×10^5 cells/mL) were seeded in a 96-well culture plate and treated with dasatinib (50 nM) and/or R406 (2 μg/mL) for 3 hours. Then, the cells were cocultured with HK yeasts and hyphae of *C. albicans* at an E:T ratio of 1:1 in a humidified atmosphere with 5% CO_2 at 37°C, and after 24 hours of incubation, the plate was centrifuged ($300 \times$ g, 10 min, 25°C), and the levels of IL-2 in the cell culture supernatants were measured by ELISA.

Apoptosis analysis using Annexin V staining

Jurkat cells modified with pLenti-mock or scFvκ3-1-CAR (2×10^5/mL) were cocultured with HK yeast or hyphae of *C. albicans* in a 96-well cell culture plate at an E:T ratio of 1:1. Arsenic trioxide (As_2O_3, 12 μM) was used as a positive control to induce apoptosis, and the cells incubated only with medium were considered a negative control. After 24 hours of incubation in a humidified atmosphere with 5% CO_2 at 37°C, 10× binding buffer was added to the cell culture prior to incubation with PE-conjugated Annexin V (2 μL/well/200 μL). After 30 minutes of incubation at 37°C, the cells were harvested, and the percentage of mock and scFvκ3-1-CAR Jurkat cells positive for Annexin V was determined by flow cytometry.

Detection of CD107a expression by flow cytometry

Nontransduced NK-92 cells and NK-92 cells expressing scFvκ3-1-CAR (5×10^5/mL) were seeded in a 96-well microplate and incubated with live *C. albicans* yeast cells at a T:E ratio of 1:100. Thereafter, monensin (2 μM) and a PE-Cy5-conjugated anti-human CD107a monoclonal antibody were added to the cells at the beginning of the coculture. PMA (50 ng/mL) plus ionomycin (1 μM) was used as a positive control to induce the release of cytotoxic granules, and NK-92 cells incubated with medium alone were used as a negative control. After 6 hours of coculture in a humidified atmosphere with 5% CO_2 at 37°C, the cells were collected, and the expression of CD107a was detected by flow cytometry.

*In vitro anti-*Candida *spp. activity of NK-92 cells expressing scFvκ3-1-CAR*

For the colony forming unit (CFU) assay, NK-92 cells (5×10^5 cells/mL) modified with or without scFvκ3-1-CAR were cocultured with live yeast cells of *C. albicans, C. tropicalis*, or *C. glabrata* at a T:E ratio of 1:100. The cocultures were incubated for 24 hours in a humidified atmosphere with 5% CO_2 at 37°C, and the samples were homogenized, diluted in sterile PBS, and plated on Sabouraud dextrose agar medium supplemented with kanamycin (50 μg/mL). The plates were incubated at 30°C for 24 to 36 hours, and the number of colonies was determined to express the fungal burden as CFU/mL. The growth of yeast cells in the absence of NK-92 cells was taken as a negative control.

To perform the XTT assay, NK-92 cells expressing scFvκ3-1-CAR (5×10^5 cells/mL) were incubated with live *C. albicans* yeast cells in a 96-well plate at T:E ratios of 1:25 and 1:50. After 4 and 6 hours of incubation in a humidified atmosphere with 5% CO_2 at 37°C, the plates were centrifuged ($800 \times$ g, 10 min, RT), and the NK-92 cells were lysed with sterile distilled water for 45 minutes. The plates were centrifuged ($800 \times$ g, 10 min, RT), and the pelleted *C. albicans* was incubated with an XTT solution (0.25 mg/mL) supplemented with menadione (1 μL). After 2 hours of incubation at 37°C, the absorbance at 450 nm was recorded by a spectrophotometer. The absorbance at 690 nm was also obtained as a reference. The calculation for hyphal damage was as follows: hyphal damage [%] = $(1 - X/C) \times 100$, where X represents the absorbance of the experimental wells and C represents the absorbance of the control wells with hyphae only.

NSG mice infected with C. albicans *and treated with scFvκ3-1-CAR-NK-92 cells*

The kinetics of the dissemination of *C. albicans* was evaluated in female (n = 10) and male (n = 10) NSG mice infected with 1×10^4 *C. albicans* yeast cells (50 μL) intravenously via the retro-orbital route. After 6, 24, and 72 hours of infection, the animals were euthanized to obtain the liver, kidney, lung, and spleen, which were homogenized in 1 mL of cold sterile PBS buffer (pH 7.2). The tissue suspensions were plated on Sabouraud dextrose agar media supplemented with kanamycin (50 μg/mL). After 24 to 36 hours of incubation at 30°C, the number of colonies was determined, and the fungal burden was expressed in CFU/g.

Male NSG mice were divided into 3 groups: untreated (n = 10), NK-92 cells (n = 17), and scFvκ3-1-CAR-NK-92 cells (n = 22). All mice were infected intravenously via the retro-orbital route with 1×10^4 yeasts of *C. albicans* diluted in 50 μL of PBS. After 3 hours of infection, a suspension of NK-92 cells expressing or not expressing scFvκ3-1-CAR (5×10^6 cells/animal) diluted in 100 μL of PBS was infused via the lateral tail vein. Untreated mice received only vehicle-treated PBS via the lateral tail vein. Mice were euthanized at 24 hours postinfection, the lung, liver, and kidney were collected aseptically, and 1 mL of cold sterile PBS buffer (pH 7.2) was added to each. The organs were immediately weighed and homogenized. Then, the tissue suspension was diluted in PBS and plated on Sabouraud dextrose agar medium supplemented with 50 μg/mL kanamycin. The plates were incubated at 30°C for 24 to 36 hours, and the fungal burden was expressed in CFU/g. Three biological replicates were performed.

scFv κ3-1 protein expression and purification

The *E. coli* strain NiCo21(DE3) was transformed by heat shock with a plasmid containing the scFv κ3-1 sequence with a His-tag at its N-terminus (Supplementary Figure 2A). After colony growth on LB agar medium containing carbenicillin (50 μg/mL), scFv κ3-1 protein expression was induced using the autoinduction method with terrific broth (TB) medium. Bacteria were cultivated at 37°C and agitated at 200 rpm until the optical density (OD) reached 0.05 to 0.1. The induction was then carried out overnight at 22°C at 200 rpm. After induction, the cells were harvested by centrifugation (4000 rpm, 20 min, 4°C), and the cell pellets were resuspended in HEPES buffered saline (HBS) buffer. Next, the samples were homogenized with 2 protease inhibitor cocktail tablets (Roche). The cells were lysed by sonication and centrifuged at 18,000 rpm at 4°C for 30 minutes to separate the insoluble and soluble fractions. The supernatants containing soluble protein were used for the purification steps.

The scFv κ3-1 protein was purified by nickel affinity (Ni-NTA) chromatography, with elution at imidazole concentrations of 30 mM, 50 mM, 100 mM, 150 mM, and 300 mM in HBS buffer. The purification efficacy was assessed by sodium dodecyl sulfate-polyacrylamide gel electrophoresis (SDS–PAGE), analyzing samples from each imidazole concentration step during elution (Supplementary Figure 2A). The gel was then stained with Coomassie blue. The expected molecular weight of the scFvκ3-1 protein is 28 kDa. The corresponding band was eluted with 100 mM imidazole (Supplementary Figure 2B), and this fraction was concentrated using a 10 kDa spin filter concentrator (Vivaspin 2-10000 MWCO) and subjected to size exclusion chromatography (SEC) using high-performance liquid chromatography (HPLC; AKTA). The column used was a Superdex 75 16/600 column. The SEC process yielded 47 fractions of 2 mL each. Fractions 11 to 20 were analyzed by SDS–PAGE, and fractions 17, 18, 19, and 20 were considered the corresponding fractions of the scFvκ3-1 protein, exhibiting a single relatively intense band at approximately 28 kDa (Supplementary Figure 2C, highlighted in red). The fractions were pooled and concentrated to 500 μL each with a 10 kDa MWCO spin concentrator column. Sodium azide 0.02% (w/v) was added to the samples as a preservative. The samples were snap-frozen in liquid nitrogen and stored at −20°C.

NMR analysis of the scFv κ3-1 protein

Nuclear magnetic resonance (NMR) analysis of the scFvκ3-1 protein was performed. The sample was spiked with 10% D_2O to reference the spectrum to a deuterium lock. The NMR analysis was conducted on a 600 MHz Bruker Avance III spectrometer, collecting a 1D proton spectrum with pre-saturation for water suppression (zgesgp, 2048 scans) at 298 K.

Glycan microarray analysis

The binding specificity of the His-tagged scFvκ3-1 protein was evaluated using 2 types of carbohydrate microarrays: (1) a microarray designated 'Fungal and Bacterial Polysaccharide Array' featuring 19 saccharides (polysaccharides or glycoproteins) and a neoglycolipid (NGL) derived from chitin hexasaccharide (Supplementary Table 2); and (2) an NGL-based sequence-defined glycan screening array composed of 672 lipid-linked oligosaccharide probes, of mammalian and non-mammalian type, essentially as previously described [28]. The complete list of probes and their sequences can be found in Supplementary Table 3.

The microarray analyses were performed essentially as described previously [29]. In brief, microarray slides were blocked for 1 hour using a blocker/diluent solution comprising 10 mM HEPES (pH 7.4), 150 mM NaCl, 1% (w/v) bovine serum albumin (Sigma 7030), 0.02% casein blocker (Pierce) and 5 mM $CaCl_2$. The scFvκ3-1 protein was added at a concentration of 150 μg/mL and incubated for 90 minutes, followed by incubation with mouse monoclonal anti-His and biotinylated anti-mouse IgG antibodies (both from Sigma and overlaid at 10 μg/mL). Biotinylated plant lectin ConA (Vector Laboratories) was used at 2 μg/mL. The final detection was performed with a 30-minute overlay of streptavidin-Alexa Fluor 647 (Molecular Probes) at 1 μg/mL. All steps of the analyses were performed at room temperature. Details of the glycan library, the generation of the microarrays, imaging, and data analysis are in the supplementary glycan microarray document (Supplementary Tables 2 and 3) in accordance with the Minimum Information Required for A Glycomics Experiment (MIRAGE) guideline for reporting glycan microarray-based data [30].

Statistical analysis

Statistical analysis was conducted using Prism 9.0 (GraphPad Software). The Shapiro–Wilk test was used to assess the normality of the data, and the homogeneity of variances was evaluated using Bartlett's test for experiments with 3 or more groups. For normal distribution experiments, analysis of variance (ANOVA) was applied with Tukey's multiple comparisons test to assess the significance of differences between groups. The Kruskal–Wallis test was used with Dunn's multiple comparisons test for experiments with a nonnormal distribution. Statistical significance was set at $P < 0.05$. The results are reported as either the mean ± standard deviation (SD) or median with interquartile range.

Results

C. albicans*-specific CAR constructs generated from distinct scFvs specific to yeast and/or hyphal forms*

C. albicans-specific CAR constructs were designed with different scFvs previously characterized to recognize the yeast and hyphae of *C. albicans* [24,26,27], and CARs—namely, scFv3-CAR, scFv5-CAR, scFv12-CAR, and scFvκ3-1-CAR—were generated. These CAR constructs and their domains are schematically represented in Figure 1A. The enhanced green fluorescent protein (EGFP) serves as a marker. The titers of the scFv3-CAR, scFv5-CAR, scFv12-CAR, and scFvκ3-1-CAR lentiviral particles were determined in the Jurkat cell line, which exhibited high titers of lentiviral particles (Figure 1A), whereas the scFvκ3-1-CAR construct exhibited a lower titer.

Jurkat cells were utilized as an initial platform for CAR studies to thoroughly characterize the function of the extracellular and intracellular domains proposed in Figure 1A, and Jurkat cells are a model to validate CAR expression, cell activation, target recognition, signaling transduction pathway, and other key processes. Therefore, Jurkat cells were modified to express scFv3-CAR, scFv5-CAR, scFv12-CAR, or scFvκ3-1-CAR, and cellular expansion was performed for 7 days prior to the enrichment of *C. albicans*-specific CAR-T cells for each construct by cell sorting. The expression level of the CAR constructs (Figure 1C) and their transduction efficiency (Figure 1D) were assessed through flow cytometry by measuring the mean fluorescence intensity (MFI) and the percentage of viable cells expressing the CAR, respectively. The percentage of Jurkat cells successfully expressing scFv3-CAR, scFv5-CAR, scFv12-CAR, or scFvκ3-1-CAR was at least 96% (Figure 1C,D).

The expression of exhaustion markers (PD-1 and TIM-3) and CD25 activation marker in Jurkat cells expressing different CARs showed no significant changes compared with nontransduced controls (Supplementary Figure 1). These findings demonstrated that Jurkat T cells expressed high levels of scFv3-CAR, scFv5-CAR, scFv12-CAR, or scFvκ3-1-CAR and did not express exhaustion markers. These modified Jurkat cells could be used to explore the functionality of *C. albicans*–specific CAR constructs against the target.

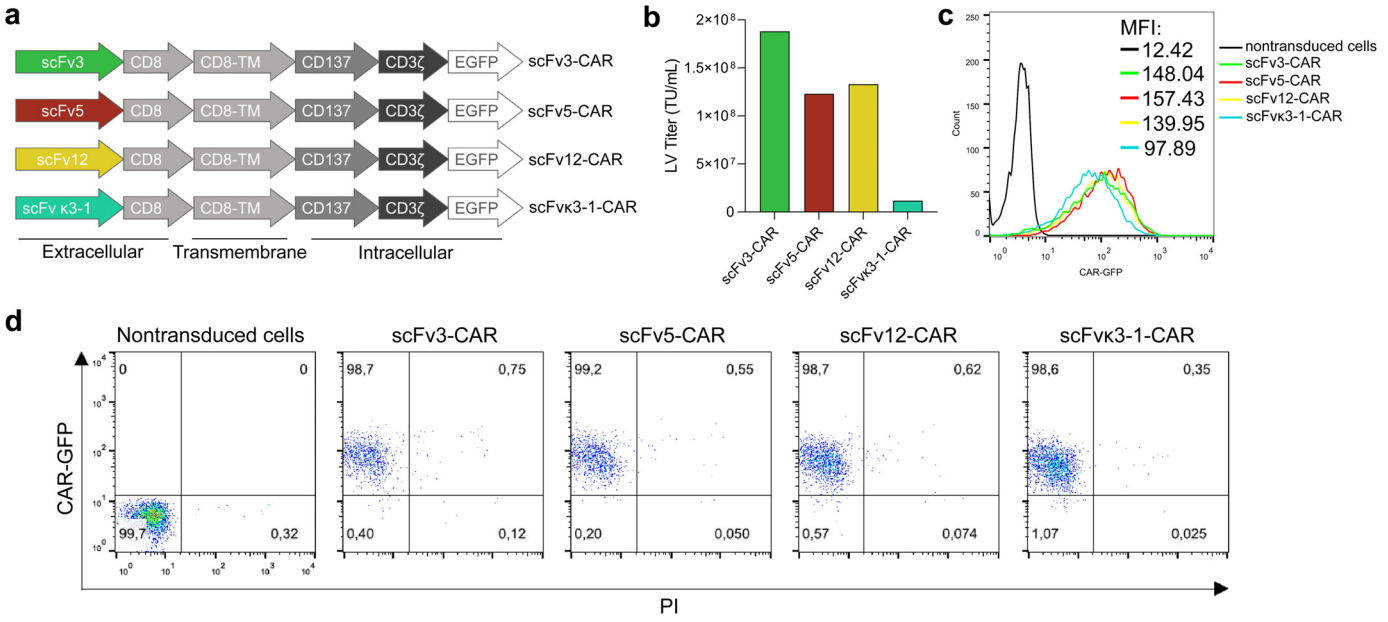

Fig. 1. scFv3-CAR, scFv5-CAR, scFv12-CAR, and scFvκ3-1-CAR are highly expressed by Jurkat cells. (A) Schematic of the domains of the scFv3-CAR, scFv5-CAR, scFv12-CAR, and scFvκ3-1-CAR constructs. (B) Quantification of the titer of lentiviral particles containing the plasmid encoding each CAR construct. Jurkat cells were used to determine the titer of the lentiviral particles produced, expressed in transducing units per milliliter (TU/mL). (C) Jurkat cells were modified with an MOI of 5 for scFv3-CAR, scFv12-CAR, and scFvκ3-1-CAR and a multiplicity of infection (MOI) of 10 for scFv5-CAR, and the histogram represents the mean fluorescence intensity (MFI) of each CAR construct. (D) Modified Jurkat cells were isolated by fluorescence-activated cell sorting; the dot plots are representative of the frequency of CAR Jurkat cells (GFP expression) and cell viability determined by propidium iodide (PI) staining. The percentage of GFP-positive CAR Jurkat cells was determined by flow cytometry; the dot plots are representative of the results. (C, D) Nontransduced Jurkat cells were utilized as a negative control. (Color version of figure is available online.)

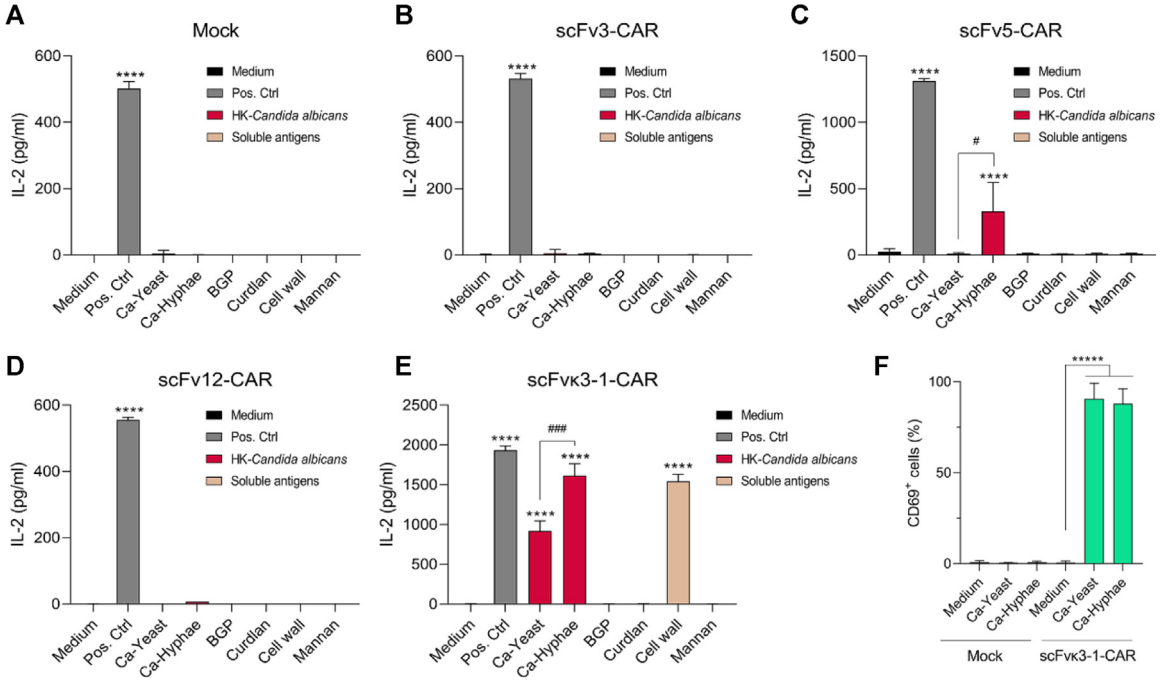

Fig. 2. scFv5-CAR and scFvκ3-1-CAR induced the activation of modified Jurkat cells in the presence of *C. albicans*. (A–F) The activation assay was performed with Jurkat cells (2×10^5 cells/mL) expressing mock (A), scFv3-CAR (B), scFv5-CAR (C), scFv12-CAR (D), or scFvκ3-1-CAR (E). The modified cells were seeded in 96-well plates and cocultured with heat-killed (HK) yeast and hyphae of *C. albicans* (1:1 ratio of target-to-effector cells) or incubated with mannan (1 μg/mL), curdlan (1 μg/mL), beta-glucan peptide (BGP; 1 μg/mL), or a cell wall extract of *C. albicans* (1 μg/mL). PMA (50 ng/mL) + ionomycin (1 μM) or PHA-L (5 μg/mL) + PMA (50 ng/mL) were used as positive controls to induce cell activation. (A–E) After 24 hours of incubation, the cell supernatant was harvested, and the levels of IL-2 were measured by ELISA (n = 3–6). (F) scFvκ3-1-CAR Jurkat cells and mock control cells were collected after 24 hours of incubation with HK yeast or hyphae of *C. albicans*, and the percentage of CD69-positive cells was detected by flow cytometry (n = 3). In (A–F), the significance was tested using one-way analysis of variance with Dunnett's test to compare each group with "medium" (*) and Student's *t*-test (#). The values are expressed as the mean ± standard deviation (SD). **** $P < 0.0001$, *$P < 0.05$, ***$P < 0.001$. (Color version of figure is available online.)

scFv5-CAR and scFvκ3-1-CAR mediated the greatest increase in cell activation in response to C. albicans *exposure*

The activation of Jurkat cells expressing scFv3-CAR, scFv5-CAR, scFv12-CAR, or scFvκ3-1-CAR in response to *C. albicans* or soluble antigens was evaluated. *C. albicans*–specific CAR-T cells were cocultured with heat-killed (HK) yeast or hyphal forms of *C. albicans* and were also incubated with cell wall extracts of *C. albicans*, mannan (α-1,6 backbone with α-1,2- and α-1,3-attached mannose side chains), beta-glucan peptide (BGP), or curdlan. After 24 hours, the cell culture supernatants were collected to measure the IL-2 levels by ELISA. Jurkat cells transduced with an empty vector containing only GFP (referred to as *mock cells*) served as the negative control (Figure 2A), whereas a positive control (PMA + ionomycin or PHA-L + PMA) was used to induce T-cell activation.

Among all the *C. albicans*–specific CAR constructs evaluated, the scFv5-CAR and scFvκ3-1-CAR induced the highest levels of IL-2 in the presence of *C. albicans* hyphae compared with those induced by the modified cells incubated with medium alone (Figure 2B–E). Additionally, scFvκ3-1-CAR induced significant amounts of IL-2 against *C. albicans* yeast and the cell wall extract (Figure 2E). These data were validated by the high levels of CD69 expressed by scFvκ3-1-CAR-T cells after exposure to yeast and hyphae of *C. albicans*, which was not observed in mock control cells cocultured with *C. albicans* (Figure 2F). However, T-cell activation against *C. albicans* or soluble antigens was not induced by the scFv3-CAR or scFv12-CAR (Figure 2B,D), whereas the scFv5-CAR showed less activation compared with the scFvκ3-1-CAR. Although scFv3-, scFv5-, and scFv12-CARs induced lower activation compared with scFvk3-1-CAR, all of these chimeric receptors were efficiently expressed on the cell surface in over 98% of the modified cells (Supplementary Figure 2).

C. tropicalis, C. glabrata, *and* C. auris *were also recognized by scFvκ3-1-CAR*

Considering the reduced ability of Jurkat cells expressing scFv3-CAR or scFv12-CAR to recognize both yeasts and hyphae of *C. albicans*, resulting in weak cell activation, subsequent assays focused on CAR constructs containing scFv5 or scFvκ3-1. The growth of Jurkat cells expressing scFv5-CAR or scFvκ3-1-CAR was monitored over time, and the cell concentration and CAR expression were determined every 2 days for 10 days. The expansion rate and percentage of GFP-positive cells did not differ between *C. albicans*–specific CAR-T cells and mock-treated T cells (Figure 3A,C). However, Jurkat cells showed reduced expression of scFv5-CAR after 7 days of culture (Figure 3B).

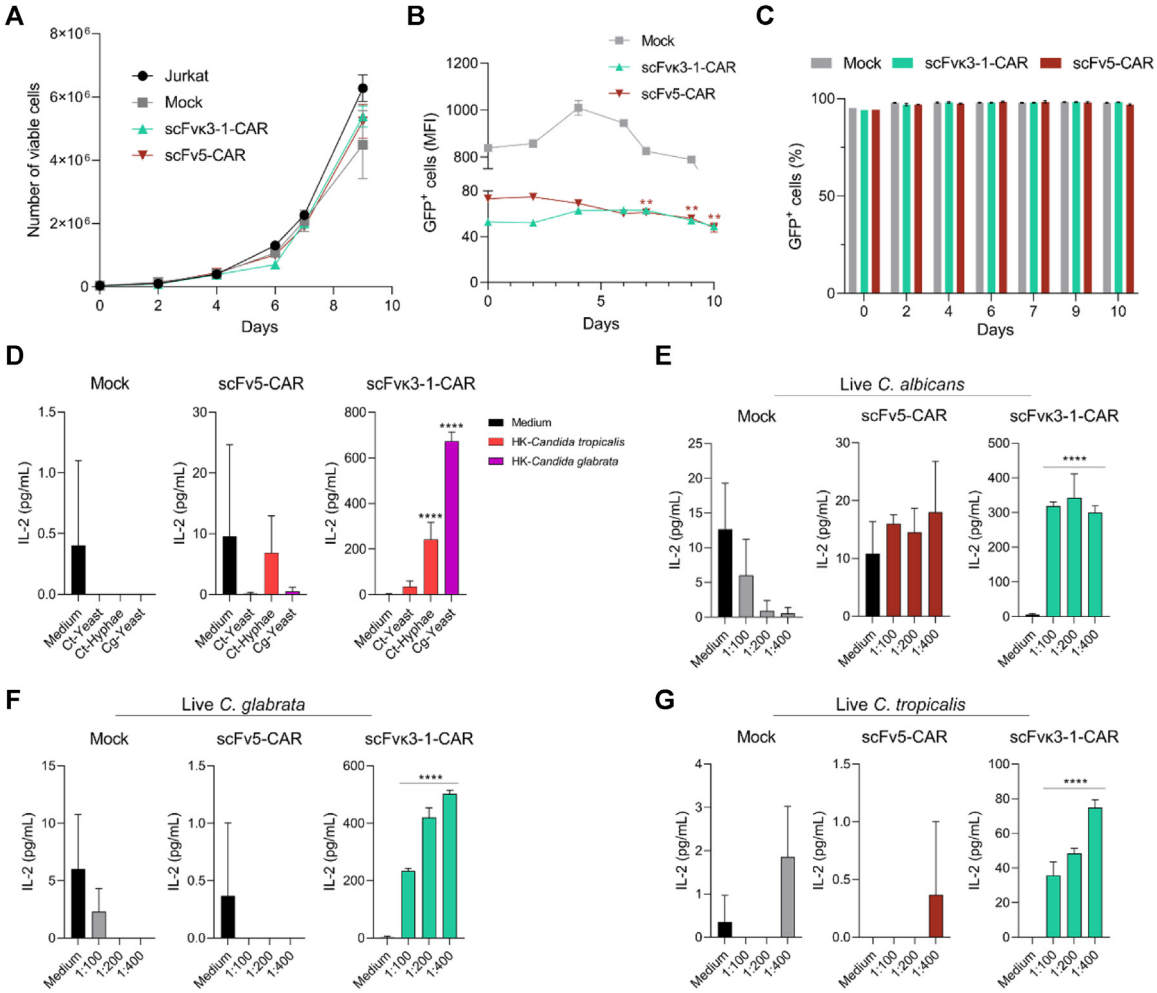

Fig. 3. scFvκ3-1-CAR Jurkat cells were activated in the presence of inactivated and live *Candida* species. Jurkat cells expressing mock, scFv5-CAR, or scFvκ3-1-CAR were cultured for 10 days to determine (A) the extent of cellular expansion, (B) the level of CAR expression, as determined by the mean fluorescence intensity (MFI), and (C) the percentage of GFP-positive cells. (A–C) n = 3–6 independent experiments. (D) Jurkat cells (2×10^5 cells/mL) expressing mock, scFv5-CAR, or scFvκ3-1-CAR were distributed in a 96-well plate and cocultured with heat-killed (HK) yeast or hyphae of *Candida* spp. (1:1 ratio of target-to-effector cells). (E–G) Modified cells were cocultured with live *Candida* spp. yeasts at different ratios of target-to effector cells (1:100, 1:200, and 1:400). (D–G) After 24 hours of incubation, the cell supernatants were collected, and IL-2 levels were measured by ELISA (n = 3). The groups of each assay were compared to "Medium." The values are expressed as the mean ± SD. $^{**}P < 0.01$, $^{****}P < 0.0001$. (Color version of figure is available online.)

The ability of scFv5-CAR and scFvκ3-1-CAR Jurkat cells to recognize different *Candida* species was determined after coculture with HK fungi. scFvκ3-1-CAR induced higher levels of IL-2 in response to yeasts and/or hyphae of *C. glabrata* and *C. tropicalis* than mock cells (Figure 3D). Moreover, scFvκ3-1-CAR-expressing cells also induced cell activation in the presence of clinical isolates of *C. auris* (Supplementary Figure 3). In addition, scFvκ3-1-CAR-expressing cells were activated in the presence of live *C. albicans* (Figure 3E), *C. glabrata* (Figure 3F), and *C. tropicalis* (Figure 3G), whereas scFv5-CAR Jurkat cells were not activated in the presence of live *Candida* spp. (Figure 3E–G). Supplementary Table 1 lists additional fungal genera—including *Cryptococcus* spp., *Aspergillus* spp., and *Rhizopus* spp.—that were cocultured with modified Jurkat cells, but fungal recognition was not detected. Taken together, these data demonstrated that scFv5-CAR recognized only the inactivated hyphae of *C. albicans*, whereas scFvκ3-1-CAR mediated T-cell activation against distinct *Candida* species.

scFvκ3-1-CAR redirected Jurkat cells to interact with C. albicans *and induced a strong cell activation*

The interaction between scFvκ3-1-CAR Jurkat cells and yeasts or hyphal forms of *C. albicans* was demonstrated through fluorescence microscopy. The absence of interaction between mock cells and *C. albicans* was evidenced by the lack of detection of yeasts or hyphae of *C. albicans* in the clusters of mock cells (Supplementary Figure 4). Conversely, scFvκ3-1-CAR Jurkat cells exhibited a strong ability to attract *C. albicans* yeast. The modified cells were in direct contact with the entire length of each hypha structure, showing that both the yeast and hyphae of *C. albicans* were targeted by scFvκ3-1-CAR (Supplementary Figure 4).

The intracellular domain of CARs initiates a signaling cascade involving ZAP-70/Syk and the Src family of tyrosine protein kinases (TPKs) upon CD3ζ phosphorylation. This signaling cascade was evaluated in scFvκ3-1-CAR Jurkat cells cocultured with HK yeasts or hyphae of *C. albicans* for 10 minutes (Figure 4A). Hydrogen peroxide (H_2O_2) was added to the cell culture as a positive control to induce ZAP-70 phosphorylation. Phospho-ZAP-70$^+$ cells were not detected in mock-Jurkat cells after incubation with *C. albicans*. However, the percentage of phospho-ZAP-70$^+$ cells in Jurkat cells expressing scFvκ3-1-CAR increased by 17.13% after coculture with yeast and by 37.59% after coculture with hyphae of *C. albicans* (Figure 4A). To further investigate the intracellular signaling triggered by scFvκ3-1-CAR, we analyzed cell activation in the presence and absence of dasatinib (Src family kinase inhibitor) and/or R406 (Syk inhibitor; Figure 4B). Dasatinib completely abrogated IL-2 production, while R406 inhibitor significantly reduced IL-2 levels (Figure 4B). Dasatinib associated with R406 further suppressed IL-2 secretion (Figure 4B). These findings indicate that scFvκ3-1-CAR activates Jurkat cells through both ZAP-70/Syk and Src family kinase signaling pathways.

To determine whether the activated scFvκ3-1-CAR Jurkat cells become exhausted after coculture with *C. albicans*, we assessed the staining with Annexin V (Figure 4C) and the expression of exhaustion and activation markers (Figure 4D). The percentage of Jurkat cells expressing scFvκ3-1-CAR and positive for Annexin V increased in the presence of yeast and hyphae (Figure 4C), whereas the percentage of Annexin V-positive mock-Jurkat cells did not increase. The cell concentration of Annexin V–negative cells was not altered (Figure 4C). In addition, scFvκ3-1-CAR Jurkat cells cocultured with the yeast or hyphae of *C. albicans* had an increased percentage of cells positive for PD-1, TIM-3, and CD25 compared with cells incubated with medium alone (Figure 4D). Thus, the strength of the signal transduction triggered by scFvκ3-1-CAR can induce the expression of exhaustion markers in response to target exposure.

The growth of C. albicans *was compromised in NK-92 cells expressing scFvκ3-1-CAR*

The functionality of the extracellular and intracellular domains of scFvκ3-1-CAR was effectively characterized using Jurkat cells, demonstrating the recognition of *Candida* species followed by robust cell activation. It made sense to select a model with intrinsic factors against fungi, NK-92 cells, to assess the ability of scFvκ3-1-CAR to mediate cell activation and effector activity to combat invasive candidiasis. Additionally, NK-92 cells are already being utilized in clinical trials for solid tumor treatment [23], making this approach promising for future clinical translation. The transduction efficiency of NK-92 cells modified with scFvκ3-1-CAR was 40.2%, with high expression levels indicated by the MFI (Figure 5A). After cell sorting, CAR expression increased to 93.8%, followed by a higher MFI (Figure 5A). Fluorescence microscopy revealed that scFvκ3-1-CAR-NK-92 cells formed clusters around live *C. albicans* yeast, suggesting specific CAR-mediated recognition, a pattern not observed in nontransduced NK-92 cells (Figure 5B). This interaction was consistent across T:E ratios of 1:50 and 1:100 (Figure 5B).

To evaluate the activation of modified NK-92 cells, the cells were cocultured with HK yeast and hyphae of *C. albicans* (Figure 6A). Compared with unstimulated cells, unmodified NK-92 cells did not show an increased production of IFN-γ in the presence of HK yeast or hyphae of *C. albicans* (Figure 6A). In contrast, scFvκ3-1-CAR-NK-92 cells produced higher levels of IFN-γ in response to HK yeast or hyphae of *C. albicans* after 24 hours of coculture than scFvκ3-1-CAR NK cells incubated with only medium (Figure 6A). In addition, NK-92 cells expressing scFvκ3-1-CAR were also activated after coculture with live *C. albicans* at T:E ratios of 1:100 and 1:200. This was evidenced by the high levels of IFN-γ released after 24 hours of incubation (Figure 6B).

To evaluate the NK cell-mediated cytotoxicity against *C. albicans*, scFvκ3-1-CAR-NK-92 cells were cocultured with live *C. albicans* at a T:E ratio of 1:100, and the release of cytotoxic granules was determined by the cell surface marker CD107a. PMA + ionomycin was used as a positive control to induce strong degranulation. Approximately 40–42% of unmodified NK-92 cells were CD107a$^+$ cells in the presence or absence of *C. albicans* (Figure 6C), whereas the percentage of CD107a$^+$ cells among NK-92 cells expressing scFvκ3-1-CAR increased significantly when the cells were incubated with *C. albicans* (73.9%; Figure 6C). Taken together, the data demonstrated that scFvκ3-1-CAR mediated strong NK-92 cell activation, suggesting the release of cytotoxic granules and IFN-γ, which are required to combat *C. albicans* infection.

The ability of scFvκ3-1-CAR-NK-92 cells to slow or inhibit the growth of *C. albicans* was investigated. Nonmodified NK-92 cells and scFvκ3-1-CAR-NK-92 cells were cocultivated with live *C. albicans* yeast at a T:E ratio of 1:100, and *C. albicans* cultivated without NK-92 cells ("*C. albicans* only") was used as a control (Figure 6D). Compared with those in the *C. albicans*–only group, the fungal burden in the scFvκ3-1-CAR-NK-92 cell group was reduced (Figure 6D). To further evaluate the fungal damage caused by scFvκ3-1-CAR-NK-92 cells after a few hours of *C. albicans* infection, a colorimetric assay was conducted using XTT. After 4 hours of incubation, the level of fungal damage did not significantly differ between the two groups (Figure 6E). However, scFvκ3-1-CAR-NK-92 cells exhibited increased fungal damage at a T:E ratio of 1:25 after 6 hours of incubation (Figure 6E). Additionally, NK-92 cells expressing scFvκ3-1-CAR were incubated with *C. tropicalis* or *C. glabrata,* and after 24 hours of coculture, the fungal burden in the two groups was unaffected (Supplementary Figure 5A,B). These data suggest that scFvκ3-1-CAR-NK-92 cells exhibit antifungal activity against *C. albicans*.

scFvκ3-1-CAR-NK-92 cells were redirected to attack C. albicans *in NSG-infected mice*

NSG mice (NOD scid gamma mice) are commonly used as preclinical models to investigate the efficacy and safety of CAR-T and CAR-NK cell therapy, as these mice lack murine T, B, NK, and functional

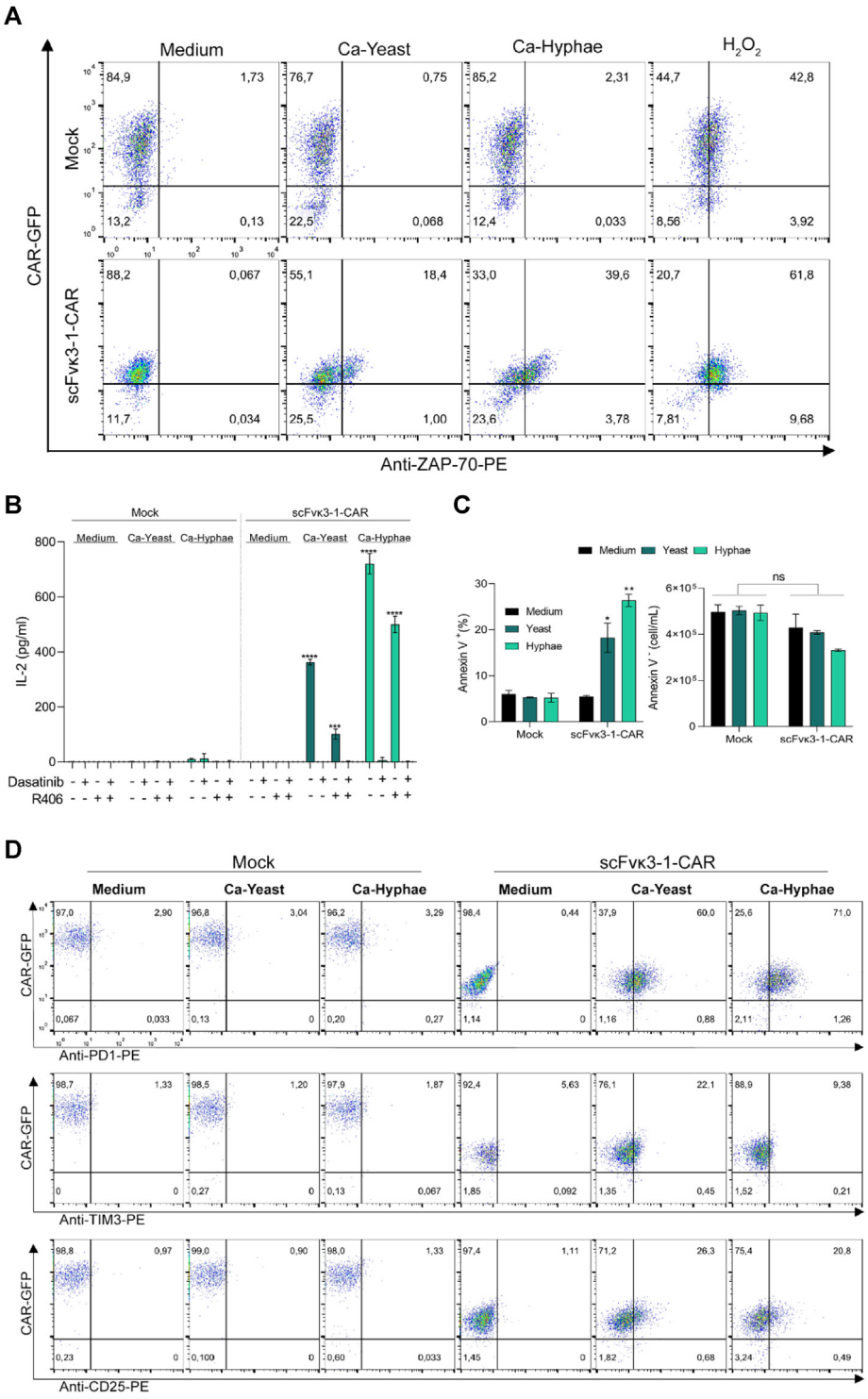

Fig. 4. Strong cell activation induced by scFvκ3-1-CAR against *C. albicans* was evidenced by positive staining for phospho-ZAP-70 and exhaustion markers. Jurkat cells (2×10^5 cells/mL) expressing scFvκ3-1-CAR or modified with the mock construct were cocultured with heat-killed (HK) yeast and hyphae of *C. albicans* in a 96-well plate at a 1:1 ratio of target-to-effector cells. (A) After 10 minutes of incubation, the cells were harvested, fixed/permeabilized, and incubated with an anti-phospho-ZAP-70-PE antibody to determine the percentage of positive cells by flow cytometry. Hydrogen peroxide (0.03%) was used as a positive control for phospho-ZAP-70. One representative experiment out of 2 is presented. (B) Modified cells were treated with dasatinib and/or R406 for 3 hours before coculture with *C. albicans*. After 24 hours of incubation, the levels of IL-2 in the cell supernatant were measured by enzyme-linked immunoassay (n = 3–4). (C) Percentage of modified cells positive for Annexin V (*left side*) and concentration of unstained cells (Annexin V^-; *right side*) after 24 hours of coculture with HK yeast and hyphae of *C. albicans* (n = 2). (D) scFvκ3-1-CAR and mock-Jurkat cells were cocultured with distinct forms of *C. albicans* for 24 hours, followed by incubation with phycoerythrin (PE)-conjugated anti-CD25, anti-PD-1, or anti-TIM3 monoclonal antibodies, and the percentages of cells double-positive for GFP and activation or exhaustion markers were determined by flow cytometry. One representative experiment out of 2 is presented. (B, C) The experimental groups were compared with the "medium" group in each assay. The values are expressed as the mean ± SD. $^*P < 0.05$, $^{**}P < 0.01$, $^{***}P < 0.001$, $^{****}P < 0.0001$. ns, not significant. (Color version of figure is available online.)

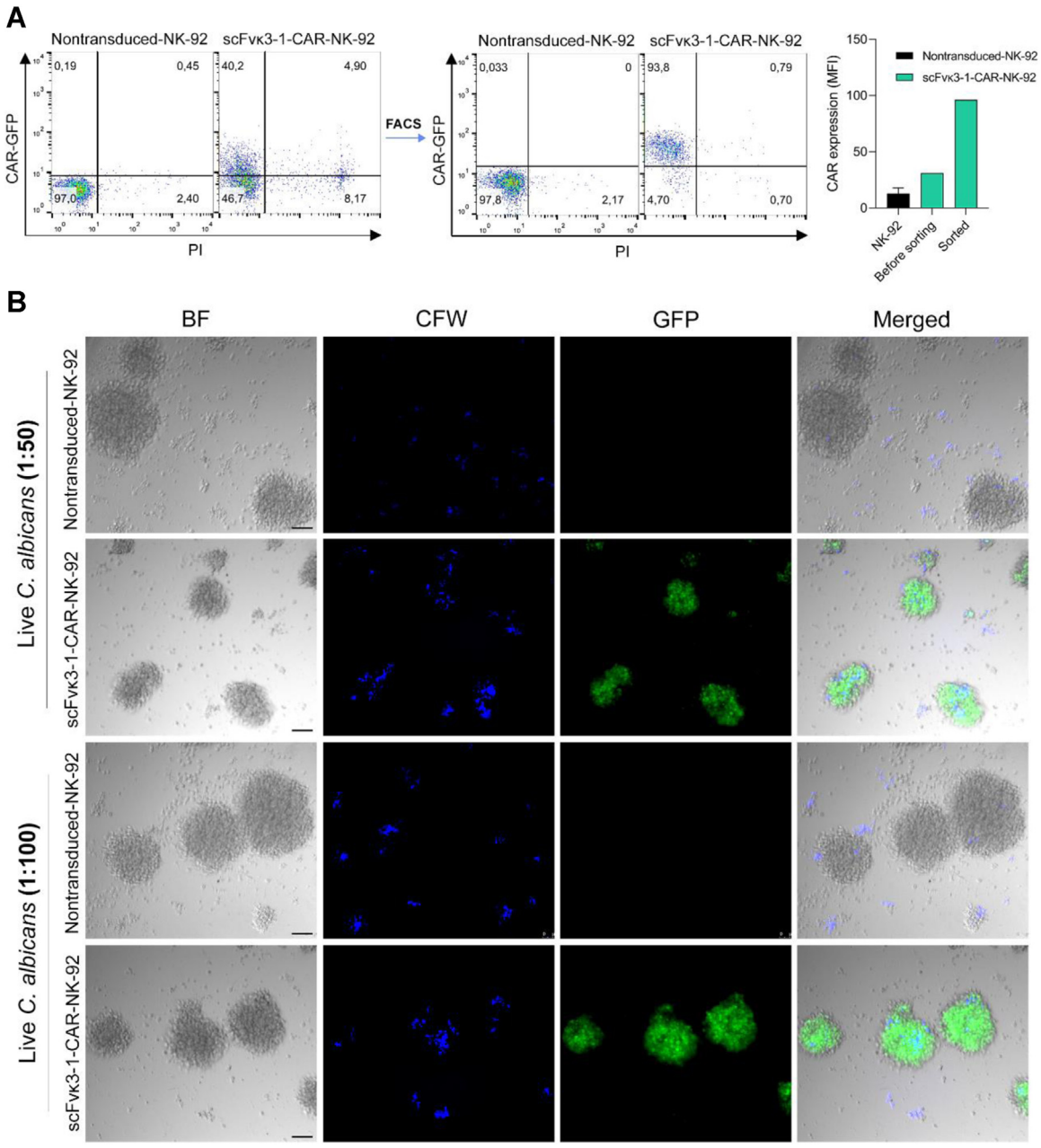

Fig. 5. scFvκ3-1-CAR redirected NK-92 cells to interact with live *C. albicans*. (A) NK-92 cells were transduced with scFvκ3-1-CAR lentiviral particles at a multiplicity of infection of 10, and the transduction efficiency was determined by GFP expression using flow cytometry. The modified cells were expanded and enriched by fluorescence-activated cell sorting (FACS). Representative flow cytometry dot plots show the percentages of scFvκ3-1-CAR-NK cells (GFP^+). Viable cells were determined by propidium iodide (PI) staining. The bar graphs show the mean intensity fluorescence (MFI) of the scFvκ3-1-CAR-expressing cells (n = 1–2). (B) NK-92 cells expressing or not expressing scFvκ3-1-CAR (5×10^5/mL) were incubated with live *C. albicans* yeast cells at a ratio of 1:50 or 1:100 (target-to-effector cells) for 6 hours. Thereafter, Calcofluor white (CFW) was added to the coculture for 15 minutes. The interaction of nontransduced cells (GFP^-) or scFvκ3-1-CAR-modified cells (GFP^+) with live *C. albicans* yeast cells (*blue*) was evaluated using fluorescence microscopy (Leica). BF, brightfield. Scale bars, 100 μM. (Color version of figure is available online.)

dendritic cells [31]. Initially, *C. albicans* infection was induced in male and female NSG mice to determine the establishment and kinetics of *C. albicans* infection in distinct tissues. For this, the NSG mice were infected intravenously with 1×10^4 *C. albicans* yeasts. The fungal burdens in the liver, kidney, lung, and spleen were measured by CFU assays after 6, 24, and 72 hours of infection (Supplementary Figure 6A). The results revealed that *C. albicans* infection was first established in the lung tissue after 6 hours (Supplementary Figure 6B). Over the subsequent 72 hours, the infection disseminated and the greatest fungal burden was observed in the kidneys (Supplementary Figure 6B). The fungal burden in the liver remained consistently low throughout all stages of infection; the fungal burden in the spleen was not affected (Supplementary Figure 6B). Interestingly, there was no difference between female and male NSG mice in the establishment and dissemination of *C. albicans* infection over 72 hours (Supplementary Figure 6B).

To evaluate the redirection of scFvκ3-1-CAR-NK-92 cells and their antifungal efficacy, NSG mice were infected with 1×10^4 *C. albicans* yeast cells. After 3 hours of *C. albicans* infection, scFvκ3-1-CAR-NK-92 cells were infused intravenously (Figure 7A). Untreated mice were infected with *C. albicans* and received only the vehicle PBS via the lateral tail vein. Another group received unmodified NK-92 cells after *C. albicans* infection (Figure 7B). Given that NSG mice are immunodeficient, the intravenous infection can rapidly disseminate to multiple

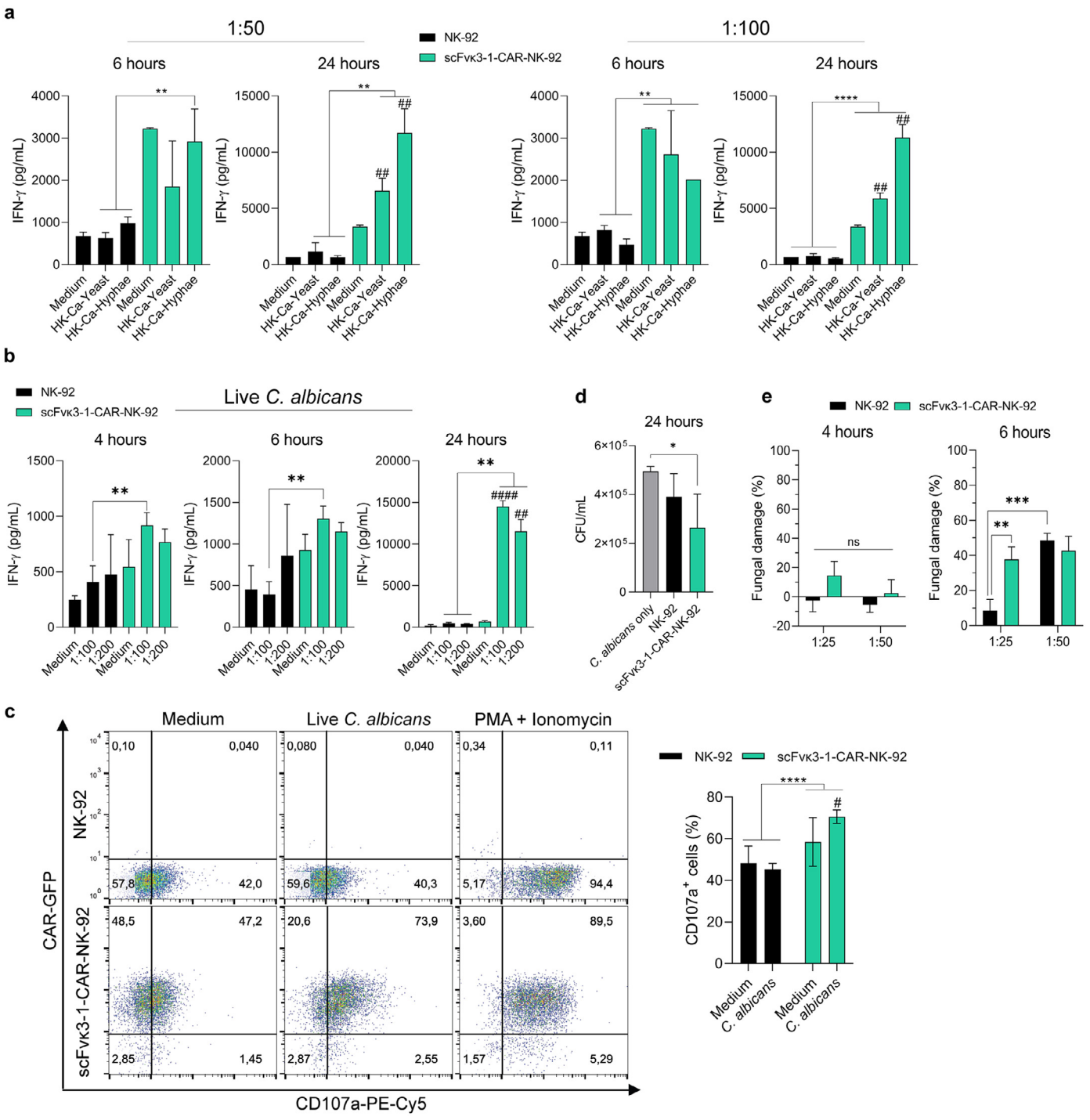

Fig. 6. scFvκ3-1-CAR-induced NK-92 cell activation affects *C. albicans* growth. (A–B) NK-92 cells expressing or not expressing scFvκ3-1-CAR were cocultured with heat-killed (HK) yeast or hyphae of *C. albicans* at a ratio of 1:50 or 1:100 (A) and live *C. albicans* yeast cells at a ratio of 1:100 or 1:200 (target-to-effector cells) (B). After 4, 6, or 24 hours of incubation, the IFN-γ levels (pg/mL) were measured by enzyme-linked immunoassay. (A,B) n = 3 independent experiments. (C) NK-92 cells modified or not with scFvκ3-1-CAR were cocultured with live *C. albicans* at a ratio of 1:100 (target-to-effector cells) in the presence of monensin and a phycoerythrin (PE)-Cy5-conjugated anti-CD107a monoclonal antibody. After 6 hours, the percentage of cells stained for CD107a was determined by flow cytometry. PMA + ionomycin was used as a positive control for degranulation induction and medium was used as a negative control (n = 4). (D,E) NK-92 cells modified or not with scFvκ3-1-CAR (5×10^5 cells/mL) were cocultivated with *C. albicans* in a 96-well plate at a ratio of 1:100 (D) or 1:25 and 1:50 (E). (D) After 24 hours, the samples were diluted and plated to perform the colony-forming unit (CFU) assay; the results are presented as CFU/mL. The *C. albicans*—only group refers to the culture of yeast with medium alone (n = 3–7). (E) After 4 and 6 hours of incubation, NK-92 and scFvκ3-1-CAR-NK-92 cells were lysed with sterile water. XTT (2,3-bis[2-methoxy-4-nitro-5-sulphenyl]2H-tetrazolium-5-carboxyanilide) solution was added and incubated for 2 hours before the absorbance reading by a spectrophotometer. The results are expressed as fungal damage (%; *n* = 3). # indicates a significant difference between the experimental group and the "medium" group of scFvκ3-1 CAR-modified cells. The values are expressed as the mean ± SD. #, $^{*}P < 0.05$; ##, $^{**}P < 0.01$; ####, $^{****}P < 0.0001$. ns, not significant. (Color version of figure is available online.)

organs, as shown in Supplementary Figure 6B, even with the low amount of inoculum used. Therefore, it was necessary to euthanize the mice 24 hours postinfection to detect an early effect of scFvκ3-1-CAR in the redirection of modified NK-92 cells considering that cell therapy was performed as a one-time treatment. The results showed a significant reduction in the fungal burden in the kidneys of the mice treated with scFvκ3-1-CAR-NK-92 cells compared with that in the kidneys of the untreated mice (Figure 7B). These findings strongly

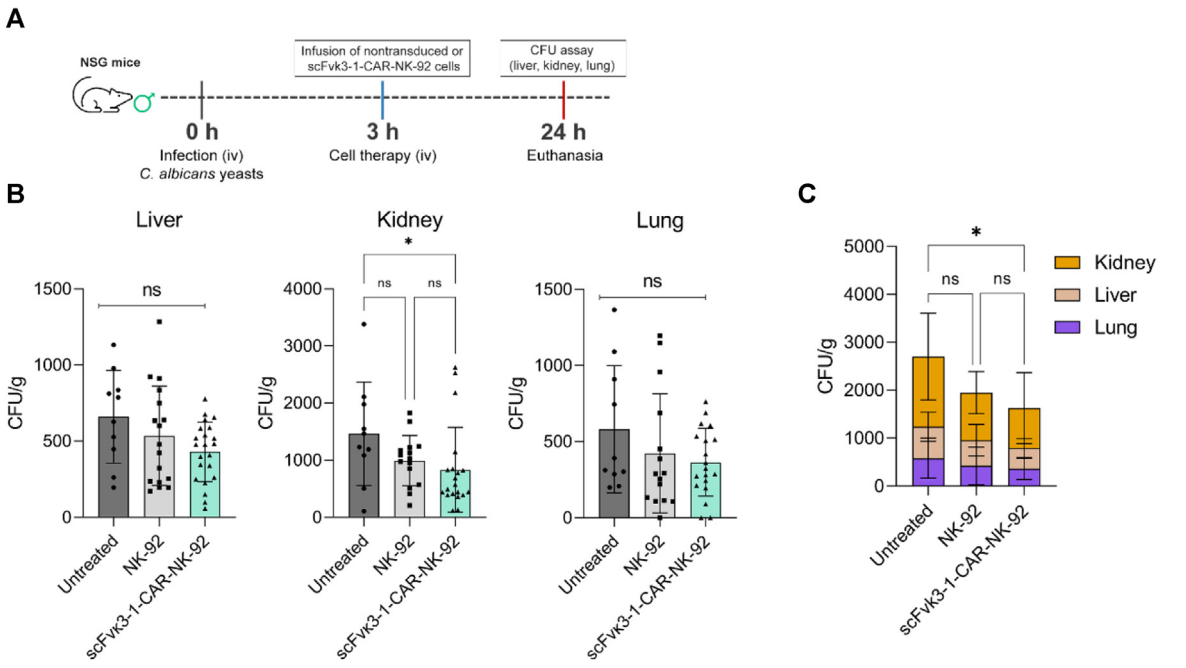

Fig. 7. NK-92 cells expressing scFvκ3-1-CAR were redirected to target *C. albicans* in the kidneys. (A) Scheme of the *in vivo* cell therapy for NSG mice infected with *C. albicans*. (A–C) Male NSG mice were infected with 1×10^4 *C. albicans* yeast cells via the intravenous route; infusion treatment occurred 3 hours after infection. The NSG mice received NK-92 cells modified or not with scFvκ3-1-CAR (5×10^6 cells/animal) via the lateral tail vein, whereas the untreated mice received only the vehicle PBS. Mice were euthanized at 24 hours post-infection and their lungs, livers, and kidneys were collected and homogenized to determine the fungal burden by CFU assay (n = 10–22). The values are expressed as the mean ± SD. $^*P < 0.05$. ns, not significant. (Color version of figure is available online.)

suggest that scFvκ3-1-CAR-NK-92 cells were redirected to combat the growth of *C. albicans in vivo*. Moreover, the kidney is a major target organ in NSG mice infected with *C. albicans* (Supplementary Figure 6B); thus, a lower fungal burden in the kidneys reinforces an early redirection potential of scFvκ3-1-CAR-NK-92 cells. In this context, the total fungal burden in all tissues combined was lower in the group treated with scFvκ3-1-CAR-NK-92 cells than in the untreated group (Figure 7C), which strengthens an early redirection of scFvκ3-1-CAR-NK-92 cells based on the cell therapy protocol, as shown in Figure 7A. In addition, the antifungal response mediated by scFvκ3-1-CAR-NK-92 cells was modest compared with data found in the NK-92 cells group. Nonetheless, basic concepts and indications of effector activity of scFvκ3-1-CAR-NK-92 cells specifically against *C. albicans* mannan were established to provide a basis for future optimization of the cell therapy protocol to enhance antifungal activity.

scFvκ3-1 has specificity for the mannan of Candida *spp*

The abovementioned findings demonstrated that scFvκ3-1-CAR successfully recognized *C. albicans* yeast and hyphae and induced Jurkat and NK-92 cell activation. scFvκ3-1-CAR incorporates an extracellular domain derived from the scFv region of a human monoclonal antibody fragment (scFvκ3-1) previously generated against *C. albicans* [27]. However, the epitope on the *C. albicans* cell wall recognized by scFvκ3-1 is unknown; carbohydrate was considered to be the possible main target [27]. To elucidate this, we generated an scFvκ3-1 protein containing a His-tag in its N-terminus using an expression vector (Supplementary Figure 7A). The scFvκ3-1 protein was expressed and purified using a nickel column, followed by size exclusion chromatography (Supplementary Figure 7B,C). The protein was then subjected to NMR analysis to corroborate its proper folding (Supplementary Figure 8). The purified scFvκ3-1 protein was used in glycan microarray experiments to determine the monosaccharide or polysaccharide ligands.

The binding of the scFvκ3-1 protein was analyzed using a glycan screening microarray containing saccharide probes, mainly polysaccharides and glycoproteins extracted from fungi and bacteria, among them mannan isolated from *S. cerevisiae* and manno-glycoproteins isolated from *C. albicans* and *A. fumigatus*. The list of the 20 saccharide probes and their sequences is in Supplementary Table 2. The scFvκ3-1 protein exclusively binds to the N-mannoprotein from *C. albicans* (probe #13) characterized by α-1,6-mannose backbone with oligomeric branches of α-1,2-, α-1,3-, and β-1,2-manno-oligosaccharides [32–34] (Figure 8). This very restricted specificity of the scFvκ3-1 is in sharp contrast with the broader binding profile of the plant lectin Concanavalin A (ConA), a plant lectin with a preference for α-linked mannose, in almost all the mannan-related probes (Figure 8). scFvκ3-1 protein was further analyzed on a broad-spectrum sequence-defined glycan screening array that contains 672 lipid-linked oligosaccharide probes, including major types of mammalian sequences that occur on glycoproteins (N- and O-linked) and glycolipids carrying various blood group ABO and Lewis antigens together with their sialylated and sulfated analogs, as well as oligosaccharide fragments of glycosaminoglycans and bacterial, fungal, and plant polysaccharides (Supplementary Table 3). The scFvκ3-1 protein exhibited no binding signals with this broad-spectrum screening array (Supplementary Figure 9), in contrast to our earlier observation of high-mannose N-glycan binding detected with C-type lectin receptors, including dectin-2 and the macrophage mannose receptor [28]. These data highlight the highly specific selective interaction of scFvκ3-1 with the N-mannoprotein of *C. albicans* without reactivity with mammalian-type glycans. Moreover, Haidaris et al. showed that scFvκ3-1 did not bind to host skin tissue in a model of cutaneous candidiasis, demonstrating its exclusive targeting of *C. albicans* without cross-reactivity [27]. Considering that our findings showed that scFvκ3-1-CAR recognized *C. albicans, C. tropicalis, C. glabrata*, and *C. auris*, it can be inferred that scFvκ3-1 may target the same or similar oligosaccharide moiety in these fungi.

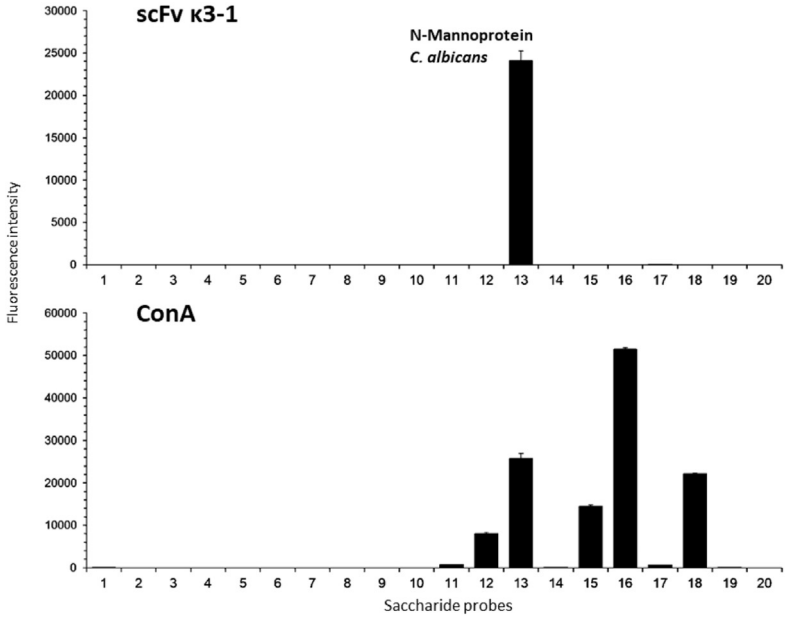

#	Probe
1	Dextran *L. mesenteroides*
2	Pullulan *P. pullulans*
3	Curdlan *Agrobacterium sp.*
4	NSG *S. cerevisiae*
5	PGG *S. cerevisiae*
6	Lentinan *L. edodes*
7	Grifolan *G. frondosa*
8	Barley β-glucan
9	Oat β-glucan
10	Lichenan
11	Pustulan *U. papullosa*
12	Mannan *S. cerevisiae*
13	N-Mannoprotein *C. albicans*
14	Mannoprotein *A. fumigatus*
15	Lipomannan *M. tuberculosis*
16	Lipoarabinomannan *M. tuberculosis*
17	Lipoarabinomannan *M. smegmatis*
18	Native O-glycoprotein *M. tuberculosis*
19	Glucurono-XyloMannan *T. fuciformis*
20	GN6-AO (neoglycolipid)

Fig. 8. Glycan microarray analysis of scFvκ3-1 and plant lectin Concanavalin A (ConA) using a focused fungal and bacterial polysaccharide array. The 20 saccharide probes are on the *right panel*, and the information on the oligosaccharide sequences is in Supplementary Table 2. The results are shown at 0.1 ng/spot (saccharides #1–19) and 5 fmol/spot (saccharide #20). The *C. albicans* N-mannoprotein, which was exclusively bound by the scFvκ3-1 protein (analyzed at 150 μg/mL), is highlighted in the *upper panel*. Values represent mean fluorescence intensities ± errors (half of the difference of signal intensities of duplicate spots for each saccharide/glycan probe). (Color version of figure is available online.)

Discussion

In recent years, the application of CAR technology in cell therapy against IFIs has shown promising results, including a notable reduction in *A. fumigatus* fungal burden *in vivo* and the modulation of virulence factors in *C. neoformans* that enable immune evasion [15–18,20]. Here, we introduced an innovative study into the application of CAR technology for the cell therapy of invasive candidiasis, marking a novel step in this emerging field. We developed four CAR constructs, scFv3-CAR, scFv5-CAR, scFv12-CAR, and scFvκ3-1-CAR, expressing these constructs in Jurkat T cells and NK-92 cells. Our results demonstrated that Jurkat cells expressing scFv5-CAR and scFvκ3-1-CAR recognized and induced strong activation in response to *C. albicans*. scFvκ3-1-CAR also recognized several clinically relevant *Candida* species, including *C. tropicalis, C. glabrata*, and clinical isolates of the emerging pathogen *C. auris*. The NK-92 cells expressing scFvκ3-1-CAR were effectively activated when exposed to *C. albicans*, resulting in notable degranulation and reduced fungal viability. Furthermore, scFvκ3-1-CAR redirected modified NK-92 cells to target *C. albicans* in NSG-infected mice. Moreover, we found that the mannan of *C. albicans* is the specific antigen recognized by scFvκ3-1-CAR without any cross-reactivity with other glycans.

In this study, we used Jurkat cells, a widely adopted model for evaluating various aspects of CAR-T cell activation, including the expression of activation markers on the cell surface, cytokine production, tonic signaling, and the expression of different CAR constructs [35,36], as previously done by our group to characterize novel CAR constructs [15–17,19]. Among the four CARs tested, only scFvκ3-1-CAR induced robust activation, whereas scFv3-CAR and scFv12-CAR failed to mediate the activation of Jurkat cells against either yeast or hyphal forms of *C. albicans*. These findings highlighted the impact of scFv stability and/or affinity on CAR performance and underscore the importance of optimizing scFv structure to enhance CAR reactivity [37–39].

The scFv5-CAR mediated Jurkat-cell activation only against *C. albicans* hyphae, whereas scFvκ3-1-CAR induced strong activation in response to both yeast and hyphal forms. This broader recognition offers several distinct advantages using immune cells expressing scFvκ3-1-CAR against *C. albicans*, especially considering the importance of the yeast-to-hyphae transition in pathogenicity [40,41]. Further experiments should be performed to investigate whether scFvκ3-1-CAR-expressing modified cells can effectively suppress this yeast-to-hypha transition in *C. albicans*, which is a limitation in this study. This approach was successfully applied using CAR-T cells to inhibit hyphal elongation in *A. fumigatus* [18], highlighting the relevance of targeting morphologic switching to reduce fungal virulence. Notably, scFvκ3-1-CAR also responded to other *Candida* species, indicating broader applicability. Previous studies indicate that *Candida dubliniensis* may also be recognized by scFvκ3-1-CAR, though further experiments are needed to confirm this [27].

Jurkat cells expressing scFvκ3-1-CAR showed strong activation upon exposure to *C. albicans*, evidenced by increased IL-2 secretion and upregulation of CD69 and CD25. Additionally, the activation of cells was validated with the upregulation of the exhaustion markers PD-1 and TIM-3, which are commonly observed as recurring indicators of cellular activation in response to target exposure and binding. Previous studies have shown that exhausted CAR-T cells are less effective at killing targets and proliferating, and PD-1 and TIM-3 expression are required to attenuate strong stimulation [42,43]. Excessive CAR signaling may explain these effects, and mutating 2 out of the 3 CD3ζ ITAMs of CAR may potentially alleviate cell exhaustion in CAR-induced T cells [44]. Importantly, scFvκ3-1-CAR includes a CD137 costimulatory domain, which is associated with superior persistence and reduced exhaustion compared with CD28-based CARs [45,46].

To evaluate antifungal efficacy, NK-92 cells were engineered to express scFvκ3-1-CAR. This cell line is widely used in CAR studies owing to its well-established cytotoxic profile [47,23,48]. Moreover, using scFvκ3-1-CAR-NK-92 cells contributes to a better understanding of the role of NK cells in invasive candidiasis, which remains complex [49,50] although their involvement in fungal burden control has been demonstrated [51]. In our model, scFvκ3-1-CAR-NK-92 cells secreted high levels of IFN-γ in response to *C. albicans* and, in its absence, suggested the presence of tonic signaling, potentially linked to high CAR surface density. A previous study from our group demonstrated a correlation between CAR expression levels and the strength

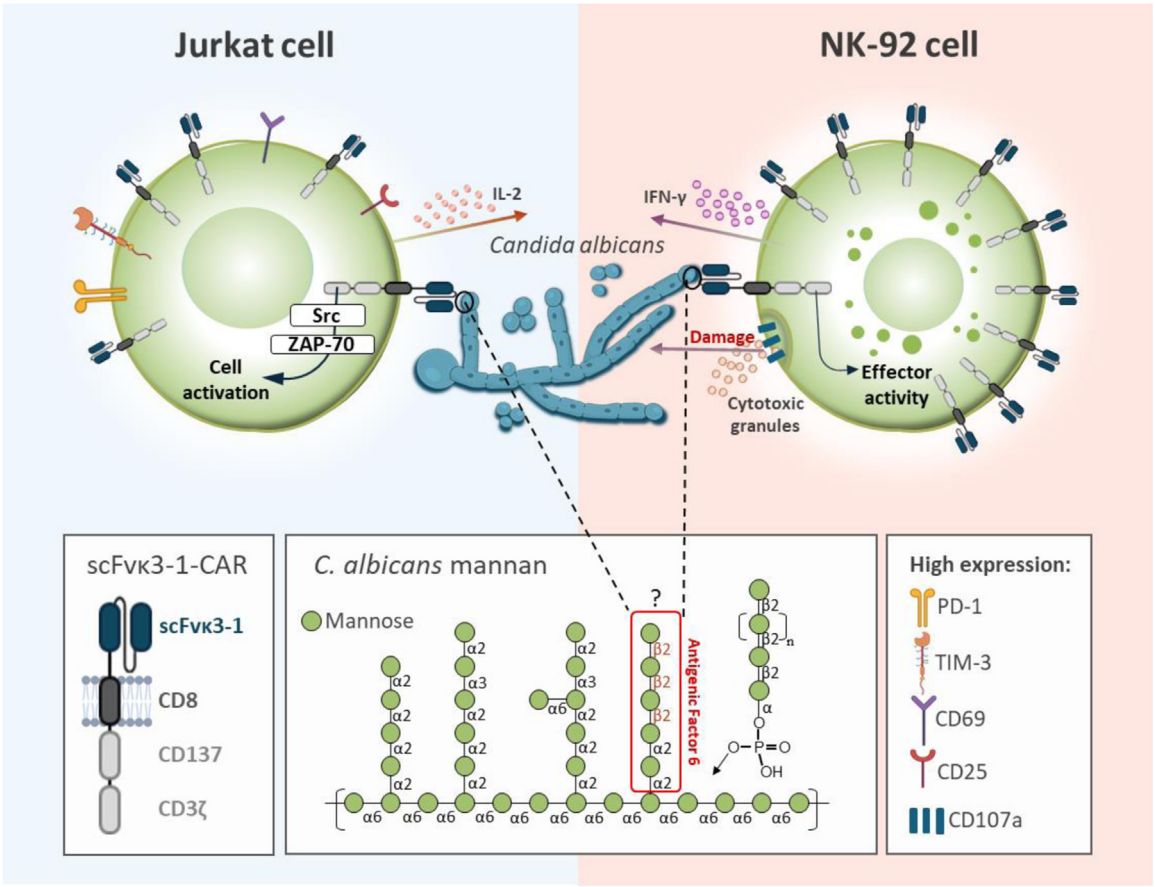

Fig. 9. Proposed model for scFvκ3-1-CAR-mediated cell activation upon recognition of *C. albicans*. The structure of scFvκ3-1-CAR comprised CD3ζ and CD137 in the intracellular domain, CD8 in the transmembrane and hinge domains, and scFvκ3-1 in the extracellular domain. Upon target recognition, scFvκ3-1-CAR mediated activation in both Jurkat and NK-92 cells. In Jurkat cells, the scFvκ3-1-CAR activation initiated a signaling cascade involving the phosphorylation of Src family tyrosine protein kinases and ZAP-70/Syk, leading to high IL-2 production and elevated expression of activation markers CD69 and CD25. These events induced an exhaustion phenotype in Jurkat cells, evidenced by the expression of exhaustion markers PD-1 and TIM-3. In NK-92 cells, the scFvκ3-1-CAR activation resulted in high IFN-γ production and elevated expression of CD107a, which is associated with increased release of cytotoxic granules. The effector activity of scFvκ3-1-CAR-NK-92 cells was demonstrated by the increased fungal damage to *C. albicans* and improved clearance in the kidneys of NSG mice. scFvκ3-1-CAR recognizes that the mannan of *C. albicans* yeast cells and hyphae, identified by glycan microarray analyses, and antigenic factor 6 (comprising 1 to 4 β-1,2-linked mannose units connected to α-1,2-linked mannotetraose [61]) is the potential moiety recognized by scFvκ3-1-CAR. (Color version of figure is available online.)

of tonic signaling [17]. which has also been associated with the T-cell expansion and maintenance both *in vivo* and *in vitro* [52,46]. Another important activation marker for scFvκ3-1-CAR-NK-92 cells is the upregulation of CD107a, which may correlate with increased perforin levels that lead to decreased metabolic activity of *C. albicans* hyphae and inhibit the elongation of *C. albicans* filaments [10,11]. Further experiments should be performed to evaluate the levels of perforin, granulysin, and granzyme B in the supernatant of scFvκ3-1-CAR-NK-92 cells cocultured with *C. albicans* to fully characterize the cytotoxic activity of these modified cells. *In vitro,* scFvκ3-1-CAR-NK-92 cells impaired fungal metabolism, as shown by the XTT assay, with greater damage observed at 6 hours than with nonmodified NK-92 cells.

This study used NSG mice as a preclinical model for invasive candidiasis, a strain commonly used to investigate the safety and efficacy of CAR-T and CAR-NK cell therapies. However, only one previous study has used NSG mice to investigate invasive candidiasis [50]. Therefore, we first established the infection kinetics in this model. Our results demonstrated initial fungal localization in the lungs at 6 hours post-infection, followed by dissemination and predominant accumulation in the kidneys by 24 hours, similar to the dynamics previously reported in BALB/c mice using bioluminescent *C. albicans* strains [53]. Based on this, we administered a single dose of scFvκ3-1-CAR-NK-92 cells 3 hours post-infection to assess the redirection of modified NK-92 cells targeting infected tissues and their potential in controlling pulmonary fungal burden and limiting dissemination. While no reduction was observed in the lungs that are an initial site of infection within the first 72 hours in NSG mice, we detected a modest decrease in kidney fungal burden in mice treated with scFvκ3-1-CAR-NK-92 cells compared with untreated animals (PBS group). This reduction was not observed in mice treated with unmodified NK-92 cells, suggesting that scFvκ3-1-CAR expression may contribute to more targeted antifungal activity in the kidneys. Moreover, animals treated with scFvκ3-1-CAR-NK cells exhibited a lower total fungal burden across all analyzed tissues. These findings support the notion that scFvκ3-1-CAR expression provides the redirection of modified cells against *C. albicans.* However, an enhanced impact of antifungal activity through CAR-based cell therapy is likely dependent on further optimization of the treatment protocol initiated in this study. Here, a single infusion of CAR-NK cells was administered, representing a key limitation in fully assessing therapeutic efficacy. Future strategies should consider multiple infusions to improve the antifungal potential of scFvκ3-1-CAR-NK-92 cells—a well-established approach in oncology—to potentially achieve greater therapeutic impact [54–56]. Although this scenario needs to be improved in this research field, our findings provide a valuable foundation for advancing CAR-NK strategies targeting the *C. albicans* cell wall, highlighting the potential of CAR technology in combating IFIs. In general, efforts to enhance CAR-based therapies for IFIs have not thoroughly addressed the safety profile of this approach, which should be considered for further experiments.

The scFvκ3-1 showed high specificity for *C. albicans* mannan without cross-reactivity to other tested glycans. This specificity was supported by previous work by Haidaris et al., which showed that scFvκ3-1 bound selectively to *C. albicans* in cutaneous infection models without detectably binding to mouse skin [27]. Importantly, scFvκ3-1-CAR recognized *C. albicans, C. tropicalis, C. glabrata*, and *C. auris*, suggesting that it targets a conserved epitope. *C. albicans, C. glabrata*, and *C. tropicalis* are known to share antigenic factor 6, defined as oligosaccharides containing 1 to 4 β-1,2-linked mannose residues attached to α-1,2-linked mannotetraose structures [57,58]. *C. auris* also has oligosaccharides containing α-1,2- and β-1,2-linked mannose units in its mannan structure [59]. Additionally, hyphal forms of *C. albicans* are enriched in β-1,2-linked mannose, which may account for the stronger binding of scFvκ3-1-CAR observed in these structures compared with yeasts [60]. Therefore, these findings support the idea that scFvκ3-1-CAR targets antigenic factor 6 within *Candida* mannan, associated with β-1,2-linked mannose residues. This recognition likely mediates the activation of both Jurkat and NK-92 cells expressing scFvκ3-1-CAR, as illustrated in Figure 9. While further studies are needed to confirm *in vivo* safety, the high target specificity of scFvκ3-1 suggests a low risk of off-target effects, reinforcing the therapeutic potential of this CAR-based approach. Thus, this study represents an important step toward evaluating the safety profile of scFvκ3-1-CAR, particularly in relation to its antigen specificity.

In conclusion, the redirection of scFvκ3-1-CAR-NK-92 cells to target *C. albicans* mannan demonstrates potential as a promising cell therapy strategy for controlling invasive candidiasis, and scFvκ3-1-CAR supports the development of distinct modified immune cells working synergistically against *C. albicans*.

Declaration of competing interest

The authors declare that there are no competing interests.

Author Contributions

GYC and TAS conceived and designed the experiments, performed the experiments, analyzed the data, prepared figures and/or tables, authored or reviewed drafts of the article, and approved the final draft. JGG, MPM, PKMOB, BS, ADM, YL, SJM, and TF performed the experiments, analyzed the data, prepared figures and/or tables, and approved the final draft. DS, PVBP, TFR, and GHG performed the experiments and approved the final draft. ASP (performed the experiments and approved the final draft).

Animal Ethics Statement

All animal experiments were approved by the Committee on Ethics in Animal Research of Ribeirão Preto Medical School (protocol 071/2021). *C. auris* (clinical isolates 467, 468, and 469) were available to make a library of GHG.'s lab, and the Committee of Ethics of the University of São Paulo, Campus of Ribeirão Preto, Brazil (Permit Number 08.1.1277.53.6; studies on the interaction of fungal pathogens with animals) approved all protocols to work with clinical isolates.

Funding

This work was supported by the Fundação de Amparo à Pesquisa do Estado de São Paulo (Grant numbers 2023/06496-0; 2022/14669-9; 2021/02758-4; 2020/16738-2; 2019/26074-7; 2018/18538-0) to TAS and GYC, and National Institute of Science and Technology in Human Pathogenic Fungi (Conselho Nacional de Desenvolvimento Científico e Tecnológico, CNPq; grant number 405934/2022-0) to GHG and TAS.

The glycan microarray studies were performed in the Carbohydrate Microarray Facility at the Glycosciences Laboratory with support from Wellcome Trust Biomedical Resource grants (099197/Z/12/Z, 108430/Z/15/Z, and 218304/Z/19/Z) and in part by the March of Dimes Prematurity research center grant (22-FY18-82). The glycan microarrays contain many saccharides provided by collaborators whom we thank, as well as members of the Glycosciences Laboratory for their contribution in the establishment of the NGL-based microarray system.

The funders had no role in study design, data collection and analysis, publication decisions, or manuscript preparation [62–64].

Supplementary materials

Supplementary material associated with this article can be found in the online version at doi:10.1016/j.jcyt.2025.05.001.

References

[1] Pappas PG, Lionakis MS, Arendrup MC, Ostrosky-Zeichner L, Kullberg BJ. Invasive candidiasis. Nature Reviews Disease Primers 2018;4. https://doi.org/10.1038/nrdp.2018.26.
[2] Denning DW. Global incidence and mortality of severe fungal disease. The Lancet Infectious Diseases 2024. https://doi.org/10.1016/S1473-3099(23)00692-8.
[3] Husni R, Bou Zerdan M, Samaha N, Helou M, Mahfouz Y, Saniour R, et al. Characterization and susceptibility of non-albicans Candida isolated from various clinical specimens in Lebanese hospitals. Frontiers in Public Health 2023;11:800.
[4] Kurrey NK, Anu-Appaiah KA, Rao RP. Probiotic yeasts inhibit virulence of non-albicans Candida species. MBio 2019;10(5). https://doi.org/10.1128/MBIO.02307-19.
[5] Bailey DA, Feldmann PJF, Bovey M, Gow NAR, Brown AJP. The *Candida albicans* HYR1 gene, which is activated in response to hyphal development, belongs to a gene family encoding yeast cell wall proteins. Journal of Bacteriology 1996;178(18):5353–60.
[6] Hoyer LL, Payne TL, Bell M, Myers AM, Scherer S. *Candida albicans* ALS3 and insights into the nature of the ALS gene family. Current Genetics 1998;33(6):451–9.
[7] Walker LA, MacCallum DM, Bertram G, Gow NAR, Odds FC, Brown AJP. Genome-wide analysis of *Candida albicans* gene expression patterns during infection of the mammalian kidney. Fungal Genetics and Biology 2009;46(2):210–9.
[8] Gow NAR, Van De Veerdonk FL, Brown AJP, Netea MG. *Candida albicans* morphogenesis and host defence: Discriminating invasion from colonization. Nature Reviews Microbiology 2012;10(2):112–22.).
[9] Ruiz-Herrera J, Victoria Elorza M, Valentín E, Sentandreu R. Molecular organization of the cell wall of *Candida albicans* and its relation to pathogenicity. FEMS Yeast Research 2006;6(1):14–29.
[10] Hellwig D, Voigt J, Bouzani M, Löffler J, Albrecht-Eckardt D, Weber M, et al. *Candida albicans* induces metabolic reprogramming in human NK Cells and responds to perforin with a zinc depletion response. Frontiers in Microbiology 2016;7(MAY). https://doi.org/10.3389/FMICB.2016.00750.
[11] Voigt J, Hünniger K, Bouzani M, Jacobsen ID, Barz D, Hube B, et al. Human natural killer cells acting as phagocytes against *Candida albicans* and mounting an inflammatory response that modulates neutrophil antifungal activity. The Journal of Infectious Diseases 2014;209(4):616–26.
[12] Misme-Aucouturier B, Albassier M, Alvarez-Rueda N, Pape PLe. Specific human and Candida cellular interactions lead to controlled or persistent infection outcomes during granuloma-like formation. Infection and Immunity 2016;85(1). https://doi.org/10.1128/IAI.00807-16.
[13] Kumaresan PR, da Silva TA, Kontoyiannis DP. Methods of controlling invasive fungal infections using CD8+ T cells. Frontiers in Immunology 2018;8(DEC):1939.
[14] Sam QH, Yew WS, Seneviratne CJ, Chang MW, Chai LYA. Immunomodulation as therapy for fungal infection: Are we closer? Frontiers in Microbiology 2018;9(JUL):357398.
[15] da Silva TA, Hauser PJ, Bandey I, Laskowski T, Wang Q, Najjar AM, et al. Glucuronoxylomannan in the *Cryptococcus* species capsule as a target for chimeric antigen receptor T-cell therapy. Cytotherapy 2021;23(2):119–30.
[16] Dos Santos MH, Machado MP, Kumaresan PR, da Silva TA. Titan cells and yeast forms of *Cryptococcus neoformans* and *Cryptococcus gattii* are recognized by GXMR-CAR. Microorganisms 2021;9(9). https://doi.org/10.3390/MICROORGANISMS9091886.
[17] dos Santos MH, Machado MP, Kumaresan PR, da Silva TA. Modification of hinge/transmembrane and signal transduction domains improves the expression and signaling threshold of GXMR-CAR specific to *Cryptococcus* spp. Cells 2022;11(21). https://doi.org/10.3390/CELLS11213386.
[18] Kumaresan PR, Manuri PR, Albert ND, Maiti S, Singh H, Mi T, et al. Bioengineering T cells to target carbohydrate to treat opportunistic fungal infection. Proceedings of the National Academy of Sciences of the United States of America 2014;111(29):10660–5.
[19] Machado MP, dos Santos MH, Guimarães JG, de Campos GY, Oliveira Brito PKM, Ferreira CMG, et al. GXMR-CAR containing distinct GXM-specific single-chain

variable fragment (scFv) mediated the cell activation against *Cryptococcus* spp. and had difference in the strength of tonic signaling. Bioengineered 2023;14(1). https://doi.org/10.1080/21655979.2023.2281059.

[20] Seif M, Kakoschke TK, Ebel F, Bellet MM, Trinks N, Renga G, et al. CAR T cells targeting *Aspergillus fumigatus* are effective at treating invasive pulmonary aspergillosis in preclinical models. Science Translational Medicine 2022;14(664). https://doi.org/10.1126/SCITRANSLMED.ABH1209/SUPPL_FILE/SCITRANSLMED.ABH1209_MDAR_REPRODUCIBILITY_CHECKLIST.PDF.

[21] Sadelain M, Brentjens R, Rivière I. The basic principles of chimeric antigen receptor design. Cancer Discovery 2013;3(4):388–98.

[22] Guimarães JG, de Campos GY, Machado MP, Oliveira Brito PKM, dos Reis TF, Goldman GH, et al. A novel mannan-specific chimeric antigen receptor M-CAR redirects T cells to interact with *Candida* spp. hyphae and *Rhizopus oryzae* spores. Bioengineered 2025;16(1). https://doi.org/10.1080/21655979.2025.2458786.

[23] Li H, Song W, Li Z, Zhang M. Preclinical and clinical studies of CAR-NK-cell therapies for malignancies. Frontiers in Immunology 2022;13. https://doi.org/10.3389/FIMMU.2022.992232.

[24] Laforce-Nesbitt SS, Sullivan MA, Hoyer LL, Bliss JM. Inhibition of *Candida albicans* adhesion by recombinant human antibody single-chain variable fragment specific for Als3p. FEMS Immunology and Medical Microbiology 2008;54(2):195.

[25] Al-Rawi N, Laforce-Nesbitt SS, Bliss JM. Deletion of *Candida albicans* SPT6 is not lethal but results in defective hyphal growth. Fungal Genetics and Biology: FG & B 2010;47(4):288.

[26] Bliss JM, Sullivan MA, Malone J, Haidaris CG. Differentiation of *Candida albicans* and *Candida dubliniensis* by using recombinant human antibody single-chain variable fragments specific for hyphae. Journal of Clinical Microbiology 2003;41(3):1152–60.

[27] Haidaris CG, Malone J, Sherrill LA, Bliss JM, Gaspari AA, Insel RA, et al. Recombinant human antibody single chain variable fragments reactive with *Candida albicans* surface antigens. Journal of Immunological Methods 2001;257(1–2):185–202.

[28] Vendele I, Willment JA, Silva LM, Palma AS, Chai W, Liu Y, et al. Mannan detecting C-type lectin receptor probes recognise immune epitopes with diverse chemical, spatial and phylogenetic heterogeneity in fungal cell walls. PLoS Pathogens 2020;16(1). https://doi.org/10.1371/JOURNAL.PPAT.1007927.

[29] Liu Y, Childs RA, Palma AS, Campanero-Rhodes MA, Stoll MS, Chai W, et al. Neoglycolipid-based oligosaccharide microarray system: preparation of NGLs and their noncovalent immobilization on nitrocellulose-coated glass slides for microarray analyses. Methods in Molecular Biology (Clifton, NJ) 2012;808:117–36.

[30] Liu Y, McBride R, Stoll M, Palma AS, Silva L, Agravat S, et al. The minimum information required for a glycomics experiment (MIRAGE) project: improving the standards for reporting glycan microarray-based data. Glycobiology 2017;27(4):280–4. https://doi.org/10.1093/GLYCOB/CWW118.

[31] Mhaidly R, Verhoeyen E. Humanized mice are precious tools for preclinical evaluation of CAR T and CAR NK cell therapies. Cancers, 2020;12(7):1915.

[32] Lowman DW, Ensley HE, Greene RR, Knagge KJ, Williams DL, Kruppa MD. Mannan structural complexity is decreased when *Candida albicans* is cultivated in blood or serum at physiological temperature. Carbohydrate Research 2011;346(17):2752.

[33] Masuoka J. Surface glycans of *Candida albicans* and other pathogenic fungi: physiological roles, clinical uses, and experimental challenges. Clinical Microbiology Reviews 2004;17(2):281.

[34] Takahara K, Arita T, Tokieda S, Shibata N, Okawa Y, Tateno H, et al. Difference in fine specificity to polysaccharides of *Candida albicans* mannoprotein between mouse SIGNR1 and human DC-SIGN. Infection and Immunity 2012;80(5):1699.

[35] Bloemberg D, Nguyen T, MacLean S, Zafer A, Gadoury C, Gurnani K, et al. A high-throughput method for characterizing novel chimeric antigen receptors in Jurkat cells. Molecular Therapy Methods and Clinical Development 2020;16:238–54.

[36] Jahan F, Koski J, Schenkwein D, Ylä-Herttuala S, Göös H, Huuskonen S. Using the Jurkat reporter T cell line for evaluating the functionality of novel chimeric antigen receptors. Frontiers in Molecular Medicine 2023;3:1070384.

[37] Fujiwara K, Masutani M, Tachibana M, Okada N. Impact of scFv structure in chimeric antigen receptor on receptor expression efficiency and antigen recognition properties. Biochemical and Biophysical Research Communications 2020;527(2):350–7.

[38] Kügler M, Stein C, Schwenkert M, Saul D, Vockentanz L, Huber T, et al. Stabilization and humanization of a single-chain Fv antibody fragment specific for human lymphocyte antigen CD19 by designed point mutations and CDR-grafting onto a human framework. Protein Engineering, Design and Selection 2009;22(3):135–47.

[39] Landoni E, Fuca G, Wang J, Chirasani VR, Yao Z, Dukhovlinova E, et al. Modifications to the framework regions eliminate chimeric antigen receptor tonic signaling. Cancer Immunology Research 2021;9(4):441.

[40] Bar-Yosef H, Vivanco Gonzalez N, Ben-Aroya S, Kron SJ, Kornitzer D. Chemical inhibitors of *Candida albicans* hyphal morphogenesis target endocytosis. Scientific Reports 2017;7(1). https://doi.org/10.1038/S41598-017-05741-Y.

[41] Saville SP, Lazzell AL, Bryant AP, Fretzen A, Monreal A, Solberg EO, et al. Inhibition of filamentation can be used to treat disseminated candidiasis. Antimicrobial Agents and Chemotherapy 2006;50(10):3312.

[42] Kouro T, Himuro H, Sasada T. Exhaustion of CAR T cells: potential causes and solutions. Journal of Translational Medicine 2022;20(1):1–10.

[43] Tomkowicz B, Walsh E, Cotty A, Verona R, Sabins N, Kaplan F, et al. TIM-3 suppresses anti-CD3/CD28-induced TCR activation and IL-2 expression through the NFAT signaling pathway. PLOS ONE 2015;10(10):e0140694.

[44] Feucht J, Sun J, Eyquem J, Ho YJ, Zhao Z, Leibold J, et al. Calibration of CAR activation potential directs alternative T cell fates and therapeutic potency. Nature Medicine, 2018;25(1):82–8.

[45] Haso W, Qin H, Zhang L, Orentas RJ, Fry TJ. CD22-targeted chimeric antigen receptor (CAR) T cells containing the 4-1BB costimulatory domain demonstrate enhanced persistence and superior efficacy against B-cell precursor acute lymphoblastic leukemia (ALL) compared to those containing CD28. Blood 2013;122(21). https://doi.org/10.1182/BLOOD.V122.21.1431.1431. 1431.

[46] Long AH, Haso WM, Shern JF, Wanhainen KM, Murgai M, Ingaramo M, et al. 4-1BB costimulation ameliorates T cell exhaustion induced by tonic signaling of chimeric antigen receptors. Nature Medicine 2015;21(6):581–90.

[47] Klingemann H, Boissel L, Toneguzzo F. Natural killer cells for immunotherapy—advantages of the NK-92 cell line over blood NK cells. Frontiers in Immunology 2016;7(MAR):91.

[48] Oelsner S, Friede ME, Zhang C, Wagner J, Badura S, Bader P, et al. Continuously expanding CAR NK-92 cells display selective cytotoxicity against B-cell leukemia and lymphoma. Cytotherapy 2017;19(2):235–49.

[49] Bär E, Whitney PG, Moor K, ReiseSousa C, LeibundGut-Landmann S. IL-17 regulates systemic fungal immunity by controlling the functional competence of NK cells. Immunity 2014;40(1):117–27.

[50] Quintin J, Voigt J, van der Voort R, Jacobsen ID, Verschueren I, Hube B, et al. Differential role of NK cells against *Candida albicans* infection in immunocompetent or immunocompromised mice. European Journal of Immunology 2014;44(8):2405–14.

[51] Charpak-Amikam Y, Lapidus T, Isaacson B, Duev-Cohen A, Levinson T, Elbaz A, et al. *Candida albicans* evades NK cell elimination via binding of agglutinin-like sequence proteins to the checkpoint receptor TIGIT. Nature Communications 2022;13(1). https://doi.org/10.1038/S41467-022-30087-Z.

[52] Lamarthée B, Marchal A, Charbonnier S, Blein T, Leon J, Martin E, et al. Transient mTOR inhibition rescues 4-1BB CAR-Tregs from tonic signal-induced dysfunction. Nature Communications 2021;12(1). https://doi.org/10.1038/S41467-021-26844-1.

[53] Jacobsen ID, Lüttich A, Kurzai O, Hube B, Brock M. In vivo imaging of disseminated murine *Candida albicans* infection reveals unexpected host sites of fungal persistence during antifungal therapy. Journal of Antimicrobial Chemotherapy 2014;69(10):2785–96.

[54] Bastin DJ, Kilgour MK, Shorr R, Sabri E, Delluc A, Ardolino M, et al. Efficacy of chimeric antigen receptor engineered natural killer cells in the treatment of hematologic malignancies: a systematic review and meta-analysis of preclinical studies. Cytotherapy 2024;27(3):350–64.

[55] Cao B, Liu M, Huang J, Zhou J, Li J, Lian H, et al. Development of mesothelin-specific CAR NK-92 cells for the treatment of gastric cancer. International Journal of Biological Sciences 2021;17(14):3850.

[56] Silvestre RN, Eitler J, de Azevedo JTC, Tirapelle MC, Fantacini DMC, de Souza LEB, et al. Engineering NK-CAR.19 cells with the IL-15/IL-15Rα complex improved proliferation and anti-tumor effect in vivo. Frontiers in Immunology 2023;14:1226518.

[57] Krylov VB, Gómez-Redondo M, Solovev AS, Yashunsky DV, Brown AJP, Stappers MHT, et al. Identification of a new DC-SIGN binding pentamannoside epitope within the complex structure of *Candida albicans* mannan. Cell Surface (Amsterdam, Netherlands) 2023;10. https://doi.org/10.1016/J.TCSW.2023.100109.

[58] Shibata N, Kobayashi H, Suzuki S. Immunochemistry of pathogenic yeast, *Candida* species, focusing on mannan. Proceedings of the Japan Academy. Series B, Physical and Biological Sciences 2012;88(6):250.

[59] Singh RK, Reuber EE, Bruno M, Netea MG, Seeberger PH. Synthesis of oligosaccharides to identify an immunologically active epitope against *Candida auris* infection. Chemical Science 2023;14(27):7559–63.

[60] Shibata N, Suzuki A, Kobayashi H, Okawa Y. Chemical structure of the cell-wall mannan of *Candida albicans* serotype A and its difference in yeast and hyphal forms. The Biochemical Journal 2007;404(Pt 3):365.

[61] Paulovičová E, Paulovičová L, Farkaš P, Karelin AA, Tsvetkov YE, Krylov VB, et al. Importance of *Candida* antigenic factors: structure-driven immunomodulation properties of synthetically prepared mannooligosaccharides in RAW264.7 macrophages. Frontiers in Cellular and Infection Microbiology 2019;9:482975.

[62] Davies G, Rolle AM, Maurer A, Spycher PR, Schillinger C, Solouk-Saran D, et al. Towards translational ImmunoPET/MR imaging of invasive pulmonary aspergillosis: the humanised monoclonal antibody JF5 detects *Aspergillus* lung infections in vivo. Theranostics 2017;7(14):3398.

[63] Dobos KM, Khoo K-H, Swiderek KM, Brennan PJ, Belisle JT, Dobos K, et al. Definition of the full extent of glycosylation of the 45-kilodalton glycoprotein of *Mycobacterium tuberculosis*. Journal of Bacteriology 1996;178(9):2498.

[64] Thornton CR. Development of an immunochromatographic lateral-flow device for rapid serodiagnosis of invasive aspergillosis. Clinical and Vaccine Immunology: CVI 2008;15(7):1095.